Review

Volatolomics for Anticipated Diagnosis of Cancers with Chemoresistive Vapour Sensors: A Review

Abhishek Sachan, Mickaël Castro and Jean-François Feller *

Smart Plastics Group, IRDL CNRS 6027, University of South Brittany (UBS), 56321 Lorient, France
* Correspondence: jean-francois.feller@univ-ubs.fr

Abstract: The anticipated diagnosis of cancers and other fatal diseases from the simple analysis of the volatiles emitted by the body (volatolome) is getting closer and closer from becoming reality. The promises of vapour sensor arrays are to provide a rapid, reliable, non-invasive and ready-to-use method for clinical applications by making an olfactive fingerprint characteristic of people's health state, to increase their chance of early recovery. However, the different steps of this complex and ambitious process are still paved with difficulties needing innovative answers. The purpose of this review is to provide a statement of the blocs composing the diagnostic chain to identify the improvements still needed. Nanocomposite chemo-resistive transducers have unique prospects to enhance both the selectivity and sensitivity to volatile biomarkers. The variety of their formulations offers multiple possibilities to chemical functionalization and conductive architectures that should provide solutions to discriminations and stability issues. A focus will be made on the protocols for the collection of organic volatile compounds (VOC) from the body, the choice of vapour sensors assembled into an array (e-nose), in particular, chemo-resistive vapour sensors, their principle, fabrication and characteristics, and the way to extract pertinent features and analyse them with suitable algorithms that are able to find and produce a health diagnosis.

Keywords: volatolome collection; vapour sensors selection; electronic nose design; features extraction; artificial neural networks; health diagnostic; chemo-resistive

1. Introduction

Cancers are a threat to humanity. According to the World Health Organization, 19.9 million new cases of cancer were diagnosed in 2020 with most of them concerning breast, prostate, lung or colorectum [1]. Furthermore, with the acceleration in population growth and social aging, the global cancer burden will continue to increase until 2045 in about 64.5% of people in Asia, 22.5% in Europe, 43.2% in North America, 69.2% in Latin America, 106.8% in Africa and 59.0% in Oceania. The number of new cases expected to be diagnosed is around 28.4 million by the year 2040 with an increase of 47% when compared with 2020. This prediction is mostly based on the growth of population and aging. But if other lifestyle factors are taken into consideration, these figures will be much higher.

Figure 1 (left) shows that the ratio between mortality and incidence is decreasing for breast, prostate and colorectum cancers but it remains high for lung, liver, oesophagus and pancreas cancers. This prediction is of course sex dependent as seen in Figure 1 (right) despite the fact that the incidence is generally larger for men than for women as far as genitals are not involved.
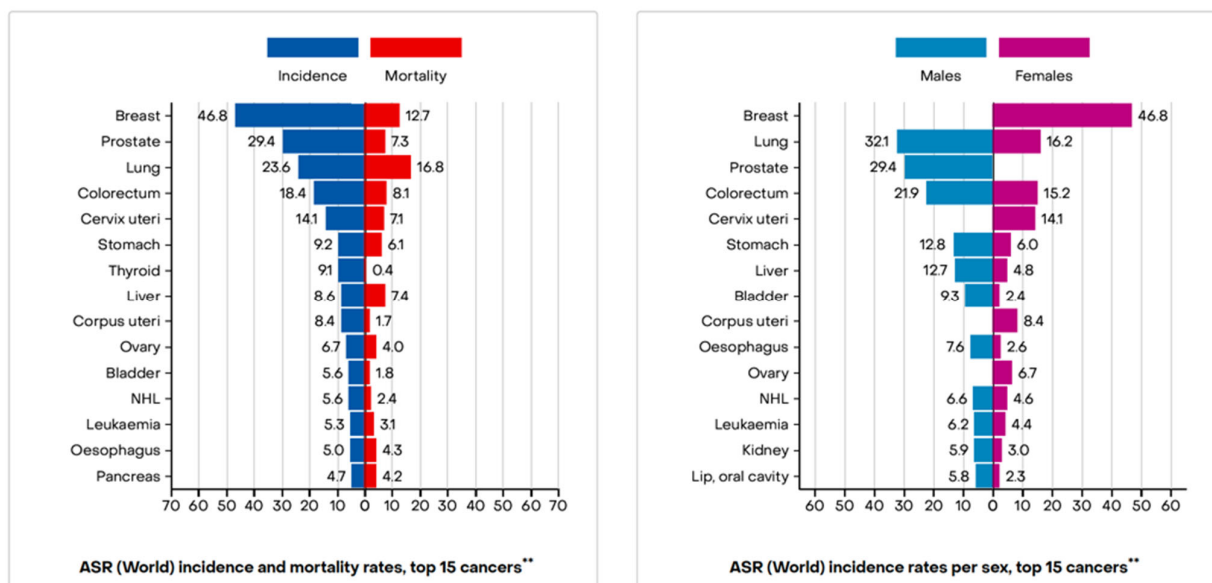
Figure 1. GLOBOCAN estimates of incidence and mortality worldwide for the top 15 cancers in 185 countries [1].

Lung cancer is the most common type of cancer which causes a huge number of deaths every year, more than any other type of cancer or disease. The survival rate of initial-stage patients is about 60 to 80% but because of current screening techniques, cancers in only 15% of patients are detected before they develop metastatic disease [2–4]. This starts in the cell lining of the bronchi and the alveoli parts of the lung. In the initial state, cells start growing rapidly but cannot be diagnosed by x-ray tests and no symptoms are shown. When cell growth causes tumours in the lung, it may spread to other parts of the body through the blood. There are two types of lung cancers: small cell lung cancer (SCLC) and non-small cell lung cancer (NSCLC). About 10–15% of cases of lung cancer are of the SCLC type. It is a very rare type of cancer for those who have never smoked. NSCLC accounts for 85–90% of the lung cancer spread in the population. Lung cancer is usually caused by tobacco smoking (active and passive), radon irradiation, exposure to asbestos fibres, air pollution, radiation therapies for other diseases, the presence of arsenic in drinking water, and a family history of lung cancer. Most of the time, lung cancer symptoms appear when the disease is in its non-curable stage. It is mainly diagnosed by sputum cytology, chest X-ray tests and Computed Tomography (CT) scans [5–7].

Skin cancer is caused by skin exposure to ultraviolet UV radiation from sunlight, and artificial UV sources such as sun lamps and tanning booths. Skin cancer is more probable in individuals with very fair skin which easily burns in the sun and those with arsenic exposure at the workplace. There are mainly two types of skin cancers: melanoma and nonmelanoma. Nonmelanoma skin cancer is also of two types, basal cell skin cancer and squamous cell skin cancer mark [8]. Melanoma skin cancer incidence rates have been increasing over the years, and it is the major cause of skin cancer deaths [9]. Patients' survival rates depend on the early diagnosis of the disease. It accounts for around 5% of all skin cancer cases in the world [10]. Nonmelanoma-type skin cancers are the most common types of skin cancer cases in the white population [11]. The nonmelanoma type of basal cell skin cancer is frequent and it usually does not spread to other body parts. Basal cell skin cancer accounts for 80% of all skin cancer cases followed by squamous cell skin cancer which accounts for 16% [12]. Therefore, melanoma is the deadliest form of skin cancer. It is curable when it is in the upper part of the skin and currently, it is examined by visual inspection of the skin, Sentinel Lymph Node Biopsy (SLNB), Positron

Emission Tomography (PET), and combined CT/PET [13]. These techniques are invasive, complicated, and require a specialist to perform and early detection is very difficult.

2. Cancer Detection

2.1. Conventional Methods

Different types of cancers present the biggest health casualties in our daily lives. Early detection of cancers is a very big challenge. The American Cancer Society (ACS) recommends an annual mammography for every woman aged above 40 years for early breast cancer detection [14]. The drawback of mammographies are that they cannot detect all forms of breast cancer and sometimes predictions may be false [15]. In some cases, additional biopsy is required which is a very painful technique and it carries the risk of fatal infections. Lung cancer, which accounts for 14% of newly detected cancer cases [16], causes the death of both men and women. For the detection of lung cancer, the chest X-ray is mostly used. But early detection of lung cancer by this method is not easy as the identification of small tumours is nearly impossible [17]. Other than that, conventional techniques are very expensive and out of reach for most of the world's financially disadvantaged population. The survival of a cancer patient depends on the stage of the cancer's detection as the earlier it is, the more chances there are to survive. Common techniques for breast, lung, and skin cancer detection are Computed Tomography (CT), Magnetic Resonance Imaging (MRI), Positron Emission Tomography, Septum Cytology, Single Photon Emission Computed Tomography, etc. [18–22]. These techniques are not fully reliable and invasive. Most of the time, patients must suffer from huge pain and unwanted radiation. Early detection of cancer is a very challenging area of research. It includes the development of chemicals and biosensors for the detection of different cancer biomarkers [22] and the design of a specialized drug delivery system for efficient treatment of cancer cells [23].

2.2. Recent Developments

Cancer screening is the most important step in its prevention and treatment. It should be diagnosed as early as possible to prevent casualties. The ACS has issued various guidelines, based on the data collected by various cancer-screening trials, for doctors and clinicians [6,24,25]. Doctors have been advised to access high-quality cancer screening and treatment facilities to diagnose patients based on their age, smoking history, habits, and health conditions. Clinicians are advised to tell their patients about future health conditions based on their current health status. A chest X-ray is not advised for the detection of lung cancer because of the radiation-associated side effects. Instead of this, Low-Dose Computer Tomography (LDCT) is suggested for adults less than the age of 74 years. LDCT has substantially reduced the deaths from lung cancer. But some drawbacks are also associated with it. LDCT can give false positive results in some diagnoses. Therefore, it requires repetitive testing and invasive methods to confirm the presence of cancer tumours in the lungs. Young patients should be screened, diagnosed, and treated for various cancers by an organized screening program with a multidisciplinary team of skilled doctors and clinicians at a high-end facility. A model study on lung cancer [26] suggested that the extension of age cancer screening from 74 years to 80 years could reduce the 14% mortality rate in lung cancer cases. Nowadays, various health organizations are issuing similar guidelines for lung cancer screening based on family history, work exposure, tobacco smoking, etc. [27–30]. Early screening for cancer is very important for saving millions of lives worldwide. Current techniques are expensive, invasive, and have a lot of complications; therefore, there is a requirement for an easy, reliable, and non-invasive technique [31]. Metabolic changes caused by cancer cells alter the production of VOC in the blood which leads to changes

in the VOC in exhaled breath [32,33]. Therefore, the anticipated diagnosis of cancer by real-time volatolome sensing can be a very useful tool [34–37].

2.3. Volatolome Analysis, a Promising Diagnosis Method

The detection of diseases using blood, body fluids, tissue testing and the direct measuring of blood samples is a primary diagnostic tool. However, the organic components of exhaled breath are directly correlated to their blood concentrations through gas exchange in the lungs. Volatile organic compounds (VOC) have been researched for many years for the diagnosis of various diseases [38]. This analysis enables the detection of biochemical processes in the body in a non-invasive way. Previously, ancient Greeks used the odour of patients' breath for the detection of some diseases. In the twentieth century, breath analysis was revolutionized by Pauling et al. who detected nearly 200 VOC in human breath using gas chromatography [39]. The combination of all of the VOC coming out of the human body is known as volatolome [40] and more than 1800 VOC have been found in human urine (279), blood (154), saliva (359), milk (256), skin (532) and breath (872) [41]. Therefore, human-exhaled breath has a health print of the body in its composition [42,43] and it can be directly related to the current condition of the lungs, asthma, and allergies [44,45]. The headspace of urine was also found to reveal biomarkers of colorectal [46] or prostate [46–48] cancers. Biomarker VOC analysis is a painless detection method and relevant screening technique for the anticipated diagnosis of cancers [49,50].

Most of the VOC in human breath are of the non-endogenous type which means these vapours cannot be utilized for diagnostic purposes. Endogenous biomarkers include hydrocarbons like ethane, pentane, and isoprene; ketones; alcohols; aldehydes; mercaptans; and amines [51]. Exhaled breath mainly contains nitrogen, oxygen, carbon dioxide, water vapours, and inert gases; therefore, the concentration of the remaining fraction is in the range of $nmol.dm^{-3}$ to $pmol.dm^{-3}$ (ppb-ppt). This concentration is also affected by the VOCs present in the environment. These VOC are termed as exogenous VOC which mainly include halogenated organic compounds. To precisely observe the metabolic or pathological process of the human body, the effect of exogenous molecules should be eliminated [52]. VOC sampling and analysis of exhaled breath should be preferred over conventional diagnosis methods as it non-invasive and potentially infectious waste is not produced during the diagnosis. This gas phase analysis is much simpler than that of complex biological tissue and blood testing [53,54].

2.3.1. Origin of VOC in the Human Body

To know the physiological and diagnosis potential of these VOC, their biological generation pathways should be well understood. Saturated hydrocarbons like ethane and pentane are produced by lipid peroxidation of ω3 and ω6 fatty acids [55]. Isoprene present in the human breath is formed by the process of cholesterol synthesis. A small fraction of exhaled isoprene is of bacterial origin and its concentration in the breath also depends on the individual's age as its concentrations are significantly lower in children [56]. Isoprene exhalation may be related to the oxidative irregularities of the fluid lining of the lung and body. Acetone is present in abundance in human breath. Acetone is generated by decarboxylation of excess Acetyl-CoA in the liver (Figure 2). Ketone concentration in the blood increases in conditions of fasting or starvation. Breath acetone concentrations are high in the case of diabetic patients [57]. Acetaldehyde is generated by the oxidation of endogenous ethanol; this is why acetaldehyde concentrations are lower than that of ethanol in the breath. The potential generation of endogenous ethanol is due to the intestinal bacterial flora [58]. 2-propanol is produced by enzymatic reduction of acetone. Methanol is produced by the intestinal bacterial presence [59]. The weakening function of the liver

causes an increase in the concentration of sulphur-containing compounds in the breath like ethyl mercaptan, dimethyl sulphide, etc. Similarly, when the lever is not able to convert the ammonia into urea, the levels of ammonia increase in the breath. This leads to an increased level of dimethylamine and trimethylamine in the breath of uremic patients [60].
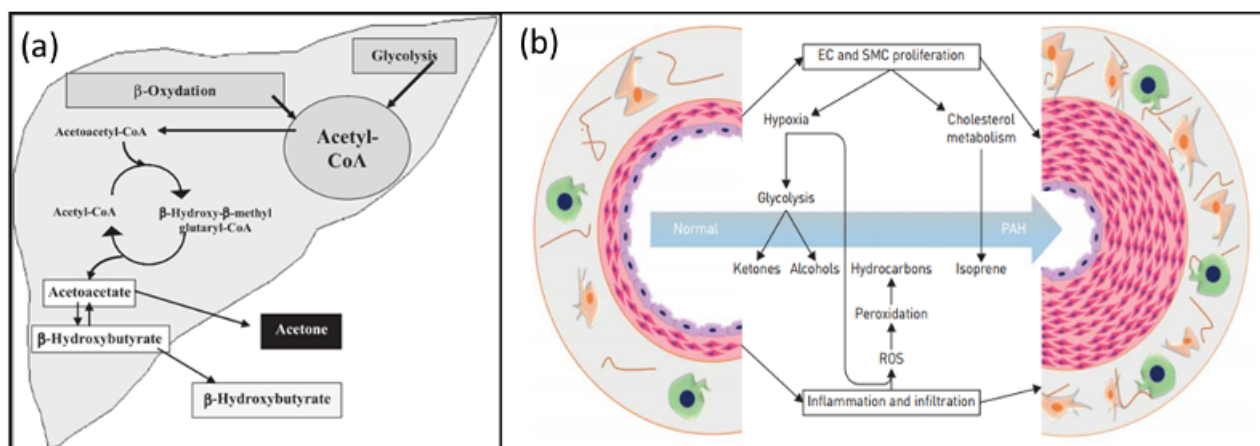

Figure 2. (**a**) Production of acetone in the liver [42]. (**b**) Production of ketones and alcohols and higher levels of isoprene in pulmonary arterial hypertension (PAH) [61].

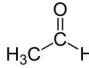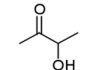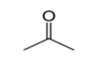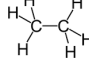### 2.3.2. Various Biomarkers of Infectious Diseases
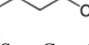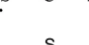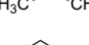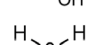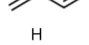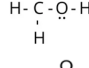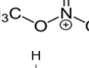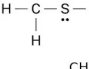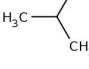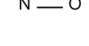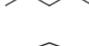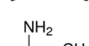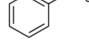
Many volatile compounds or metabolites have been identified as biomarkers for *many infectious diseases and cancer diagnoses [62]. Some biomarkers are common in two or more than two diseases. This may be due to the similar effects caused by pathogens or infections in the biochemical pathways of the human body. In some cases, physiological conditions are responsible for the generation of biomarkers. Some volatile biomarkers such as acetone, isoprene, methyl mercaptan, and dimethyl sulphide are common in many diseases [63,64]. Therefore, the presence of a certain biomarker in exhaled breath indicates the general diseased condition of a person which should be further deeply analysed. Nevertheless, it can provide rapid and easy detection of diseased conditions in the human body. Table 1 illustrates some examples of biomarkers and their related diseases [65].

2.3.3. Lung and Skin Cancer Biomarkers

Recently, cancer-related biomarker analysis in human breath has been vastly researched [66]. By examining the exhaled breath, VOC profile lung cancer prediction can be performed easily. This will lead to the development of a rapid detection technique that can detect lung cancer even in early and curable stages. Many investigations have been carried out to distinguish between VOC patterns in the exhaled breath of cancerous and noncancerous persons. Some compounds have been found that are present only in the breath of lung cancer-affected persons. Most of them are alkanes and methylated alkanes [19,67,68]. Lung cancer VOC mainly include styrene, decan, isoprene, benzene, undecane, hexane-1, hexanal, propyl benzene, 1,2,4-trimethyl benzene, heptanal and methyl cyclopentane [69].

Similarly, many VOC have been synthesized in the process of human metabolism. Many of these VOC are released by the skin as the skin has the largest surface area in the body to interact with the environment and transfer body heat, sweat, and VOC [70,71]. Acevedo et al. [72] have shown using SPME and GCMS that different types of VOC have been released from human skin cell culture over a period due to cell metabolism. VOC like benzaldehyde, styrene, benzyl alcohol, acetophenone, and dimethyl benzene were recognized in a study of human skin cell culture [73].

Table 1. List of some biomarkers for various diseases.

Biomarker	Structure	Disease/Disorder/Condition
Acetaldehyde		AFDL, URTI
Acetoin		Lung cancer, NSCLC
Acetone		ARDS, lung cancer, CIP, CPD, diabetes mellitus, hepatic cirrhosis, starvation, PLC
Ethane		AHI, asthma, COPD, cystic fibrosis, lung cancer, oxidative stress, schizophrenia
1-butanol		Lung cancer, NSCLC
Carbon disulphide		Cystic fibrosis, schizophrenia
Dimethyl sulphide		Lung cancer, hepatitis, cystic fibrosis, hepatic cirrhosis, hepatic coma
Ethanol		CPD, cystic fibrosis, diabetes mellitus
Hydrogen sulphide		Endocarditis, hepatic cirrhosis
Isoprene		AFDL, ARDS, asthma, cystic fibrosis, lung cancer
Methanol		Cystic fibrosis, lung cancer
Methyl nitrate		Diabetes mellitus, hyperglycaemia
Methyl mercaptan		Chronic hepatitis, endocarditis, hepatic cirrhosis, hepatic coma
Isobutene		Breast cancer, IHD, lung cancer, oxidative stress
Nitric oxide		Asthma, COPD
Pentane		AHI, ARDS, asthma, CIP, cystic fibrosis, lung cancer, schizophrenia
Propane		Cystic fibrosis, IBD
o-Toluidine		Lung cancer, PLC

Disease abbreviations: AFDL—alcoholic fatty liver disease, AHI—alcohol-induced hepatic injury, ARDS—acute respiratory stress syndrome, CIP—critically ill patients, CPD—cardiopulmonary disease, COPD—chronic obstructive pulmonary disease, IBD—inflammatory bowel disease, IHD—ischemic heart disease, PLC—primary lung cancer, NSCLC—non-small cell lung cancer, and UTRI—upper respiratory tract infection [65].

2.3.4. VOC Sensing: A Non-Invasive Method

Exhaled breath testing is a very useful diagnostic tool for various medical conditions. Human breath is a complex blend of numerous VOCs. This screening method can reduce the mortality rate of cancer patients [74,75]. The exhaled analysis also leads towards fast detection of certain dysfunctions in body organs like diabetic patients having an acetonic smell in their breath, a rotten fish-like smell for liver diseases, and a urine-like smell in the case of kidney disorders [76]. Increased levels of a specific biomarker indicates the medical condition of a person such as ammonia for hepatitis, alkyl amines for uraemia, and dimethyl sulphide for liver damage. Therefore, breath analysis is an outstanding method to anticipate various lung and stomach diseases [77]. For skin cancer, it is reported that dogs can smell melanoma-infected skin [78,79]. Therefore, it is suggested that cancer cells

in the skin release some VOCs which are somehow different from normal skin. D'Amico et al. [80] used GC–MS and a gas sensor array to differentiate between melanoma and normal skin. Propanal was suggested as a potential VOC that evolved from cancerous skin. Jae Kwak et al. [81] also analysed cancerous skin using GC–MS and gas sensors. They used single-strand DNA coated with carbon nanotubes (DNA CNT) to analyse the VOCs released from both types of skin and isoamyl alcohol was found at a higher amount in cancerous skin. Abaffey et al. [82] analysed VOCs obtained from fresh biopsied tissues of melanoma skin using a headspace solid-phase microextraction (HS SPME) via GC–MS. They found increased levels of lauric and palmitic acid in melanoma skin. This increased level of fatty acids is because of upregulated de novo lipid synthesis which is a characteristic of cancer. Many genetically occurring biomarkers are also recognized to detect this deadly skin cancer [83].

The concentration pattern (breath print) of these VOCs can be related to the specific health conditions of patients and can be used in anticipated diagnoses. The composition of breath can be altered by any change in metabolic and physiological activities of various body organs such as the liver [84], lung, prostate, skin [72,85,86] and kidney [87,88]. Therefore, this non-invasive diagnosis technique can detect all types of diseases, for example, liver disease, Parkinson's disease, kidney failure, tuberculosis, and cancers [89–97]. The interest of VOC sensing is not only useful for medical applications but also for environmental monitoring such as toxic gas detection and air quality monitoring (solvent vapor detection in the air) [98–102], food quality assurance [103–106], homeland security measures, beverage quality monitoring [107,108], process control in the chemical industry [109] and most importantly, in automobile emission control [110,111]. Among all these applications, industrial workplace exposure and environmental monitoring are very demanding areas for such fast and robust sensors to detect the very low concentrations of toxic VOCs and gases which are hazardous even at these concentrations [112,113]. Chemical sensors are also required for explosive detection and crime scene (forensic) investigation [114].

2.3.5. Breath Collection Methods

Breath collection is an important step in its analysis. In breath collection procedures, test subjects or patients exhale via a disposable mouthpiece with a rebreathing valve in the breath collecting unit (BCU). Water condensation is avoided by heating all gas carrying surfaces above 50 °C. Such a BCU is provided by Ionimed Analytik GmBH (Innsbruck, Austria) [115]. Breath is also collected in breath bags made of various plastic materials such as transparent Tedlar (polyvinyl fluoride) bags, black-layered Tedlar bags, FlexFoil bags, Teflon bags, and Nalophan bags [116,117]. Tedlar bags are widely used because they have a low cost, are easy and require simple handling. These bags have a drawback of inferior storage qualities compared to other bag materials [118]. Most of the time, there is no standard procedure for VOC sampling from exhaled breath, but some protocols are shown in Figure 3. The total breath can be exposed to an e-nose after collection in a bag (a) or the e-nose can be inside the container (b). Alveolar breath is more complex to collect (c) [37]. For analytical purposes, alveolar breath can be distinguished from nonalveolar breath using expired CO_2 concentrations [119].
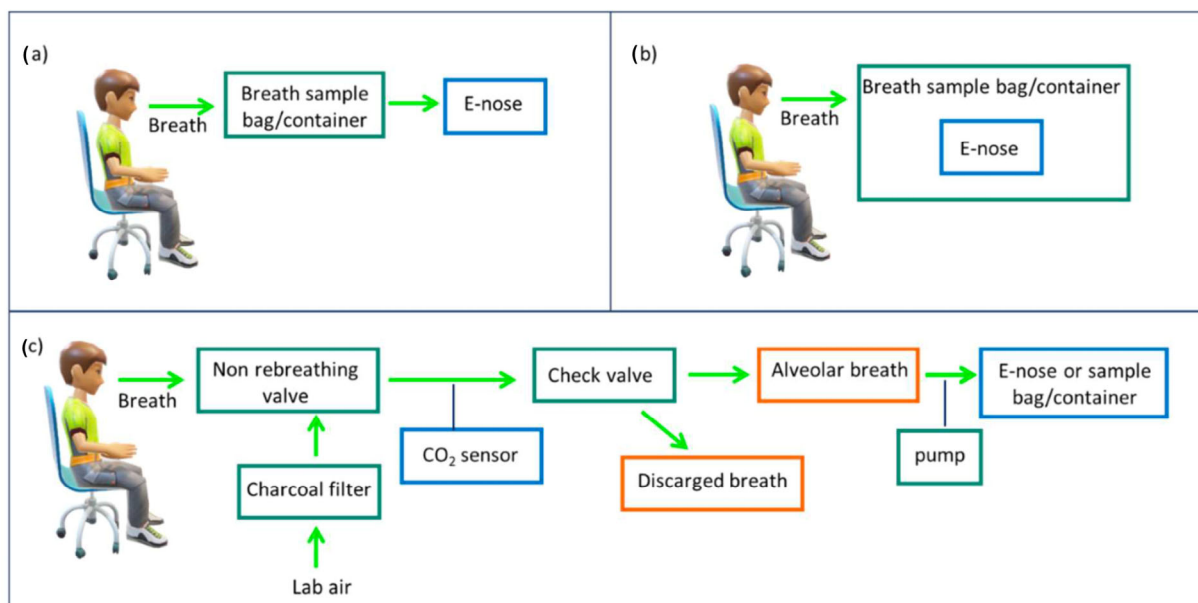
Figure 3. Different protocols allowed to collect either the total breath (**a**,**b**) or only the alveolar breath (**c**) [37].

VOC concentration in the exhaled breath is in the range of ppm to ppb level; therefore, a small amount of impurity or irregularity during the sample collection can affect the analytical results drastically. Most of the time, samples obtain impurities from inspired air or they become diluted from the dead space air [120]. Breath sampling without a controlled respiratory phase can change the original concentration of the breath collected [121]. Breath collection can be carried out in two ways: first is a mixed respiratory sampling and the other is alveolar sampling. The first one is simpler and frequently used, in which no additional equipment is required. On the other hand, alveolar air sampling provides a 2–3 times higher concentration of VOCs in comparison to mixed expiratory sampling. In many experiments, exhaled breath is collected in breath bags and is preconcentrated before testing. Sometimes instead of Tedlar bags, stainless steel electropolished canisters are used for sampling [122].

Preconcentration of samples is carried out with special adsorption materials or by direct cryofocussation [123,124]. The use of adsorption traps, coated fibres (SPME) and cryofocussation leads to an easy assessment of the breath VOC profile. For this purpose, organic polymers (Tenax TA), activated charcoal, different types of graphitized carbon (Carbopack X), and carbon molecular sieves (Carbozen 1021) have been utilized [125,126]. Human breath contains large amounts of water which should be taken into consideration to avoid any kind of damage to the instruments or errors in results. To remove water from breath samples, multibed sorption traps are used in the preconcentration step. These multibed sorption traps are composed of graphitized carbon and carbon molecular sieves. Removal of water from breath is also performed with SPME which is made of polymeric fibres. Due to the physical properties of the fibre, they can absorb a variety of VOCs on their surface and easily desorb them by heating the SPME in chromatographic analysis [127]. Tedlar bags in combination with SPME are also used for sampling and preconcentration. In such a case, alveolar breath is collected in a 1 dm^3 Tedlar bag, 200 cm^3 gas is transferred in another bag and the SPME fibre is introduced through the septum of the bag. After 15 min of absorption time, the fibre is taken out for GC analysis.

2.3.6. Skin Headspace Collection Method

To collect VOC from the skin, Turner et al. [128] used Nalophan bags as shown in Figure 4. A Nalophan bag of 4 dm^3 volume was clamped around the hand of a patient with a plastic tie and filled with clean air. Seven min equilibrium time was given for VOC emitted from the hand to be mixed with the clean air of the bag. After that, the VOC were analysed using the SIFT/MS method.

Figure 4. The sampling bag attached to the arm and the setup for SIFT-MS analysis of skin volatiles [128].

2.3.7. Analysis of Exhaled Breath

Exhaled breath is a complex mixture of 600 plus endogenous and exogenous VOCs. Some of them are generated in the body as byproducts of various metabolic processes and others are present due to environmental conditions and behavioural factors such as smoking and drinking [129,130]. Analysis of this complex VOC mixture is difficult because of their mutual interaction; therefore, a wide range of analytical techniques have been used for this purpose such as Mass Spectroscopy, Gas Chromatography–Mass Spectroscopy (GC–MS), Proton-Transfer-Reaction Mass Spectroscopy (PTR-MS), Selected-Ion Flow-Tube Mass Spectroscopy (SIFT-MS), Tuneable Diode Laser Spectrometer (TDLS), Time-of-Flight Mass Spectroscopy (TOF MS), etc. [131–133]. These techniques give very accurate results but have some disadvantages like high cost, bulky and sophisticated machinery, complicated software, and a specialist person who is required to have all the technical and maintenance knowledge. All these problems restrict their clinical widespread application. For this purpose, simple, inexpensive, and real-time breath monitoring techniques are required. In the last decade, various types of gas sensors have been developed for this purpose. These sensors provide simple non-invasive analysis and ease of handling [134–136]. The sensors developed so far are only focused on widely studied volatiles such as nitric oxide, oxygen, ammonia, acetone, and carbon di/mono oxide. These sensors are not useful in the analysis of disease biomarkers [137–139]. These sensors have been utilized by chemical, pharmacological, and food processing industries. Different types of materials have been developed recently for this purpose such as metal oxide nanoparticles, carbon nanotube-base composites, organic dielectrics, organic conductors, etc. [140]. Liao et al. [141] have used tetra thiafulvarene (TTF)- tetra cynoquino dimethane (TCQN), a highly conductive oregano metal for sensing NO$_2$ and oxygen. This was an example of irreversible sensing

because of the reaction between the gas and sensor compound. Peng et al. [142] have used a random network of single-wall carbon nanotube (RN-CNT)-based field-effect transistors (FET) for the detection of lung cancer and kidney disease from exhaled breath analysis. Figure 5a shows the schematic of RN-CNT FET and Figure 5b shows the difference in the PCA pattern of healthy and diseased humans under different relative humidity conditions of breath.
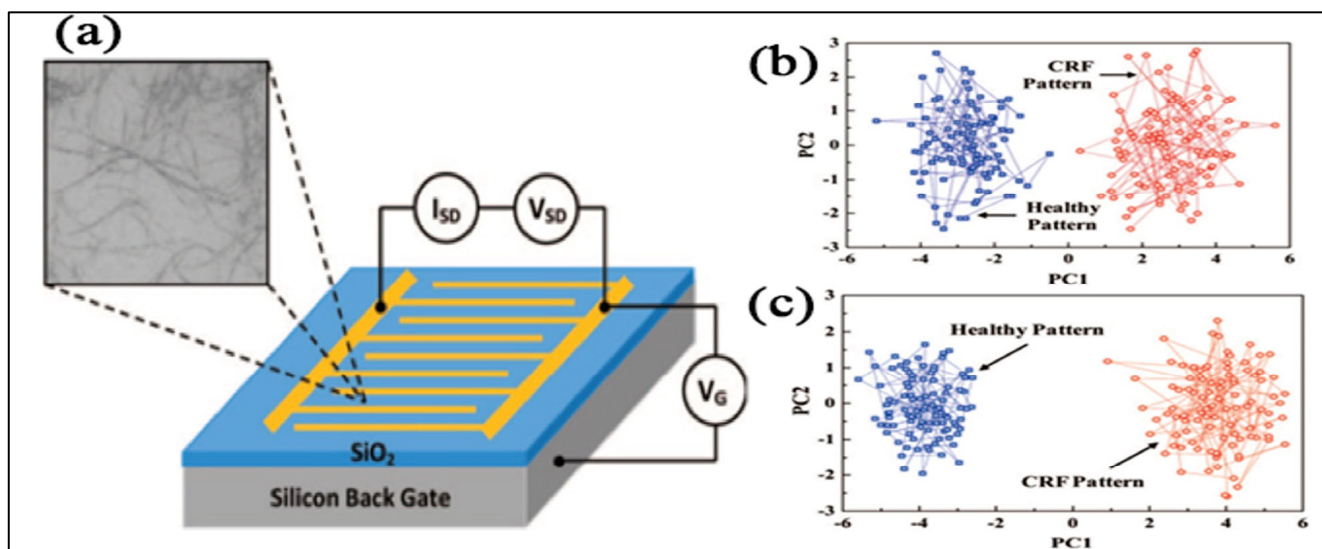
Figure 5. (**a**) Schematic representation of the RN-CNT test devices as a FET or as a chemo-resistor. The inset shows a scanning electron micrograph of the CNT random network, which connects the electrodes and forms multiple paths between them [142]. Principal component score plots of the sensor array upon exposure to simulated "healthy" and "diseased" patterns at (**b**) 80% RH and at (**c**) 10% RH.

Righettoni et al. [143] have used silicon-doped WO_3 nanoparticles for the detection of acetone in the breath of diabetes patients under ideal and real experimental conditions. They have found that the level of acetone is less than 900 ppb in healthy humans and above 1800 ppb in diabetes patients. Therefore, these materials have proved their ability as a gas sensor and further functionalization of these materials can improve their sensing properties. New possibilities have evolved with nanotechnology.

This can lead to the development of breath sensors which can overcome all the drawbacks of complex spectroscopic analysis. Devices made from these chemical sensors will be compact, lightweight, require less energy, be easy to operate, accurate, reliable, reproducible, and completely non-invasive [144]. As shown in Figure 6, Arakawa et al. have presented two methods for breath analysis. In the first method, exhaled breath is stored in a gas sampling bag and analysed when required and in the second method, breath is tested online with a gas flow controller. The second method is more appropriate for breath ethanol analysis as they have suggested [145].
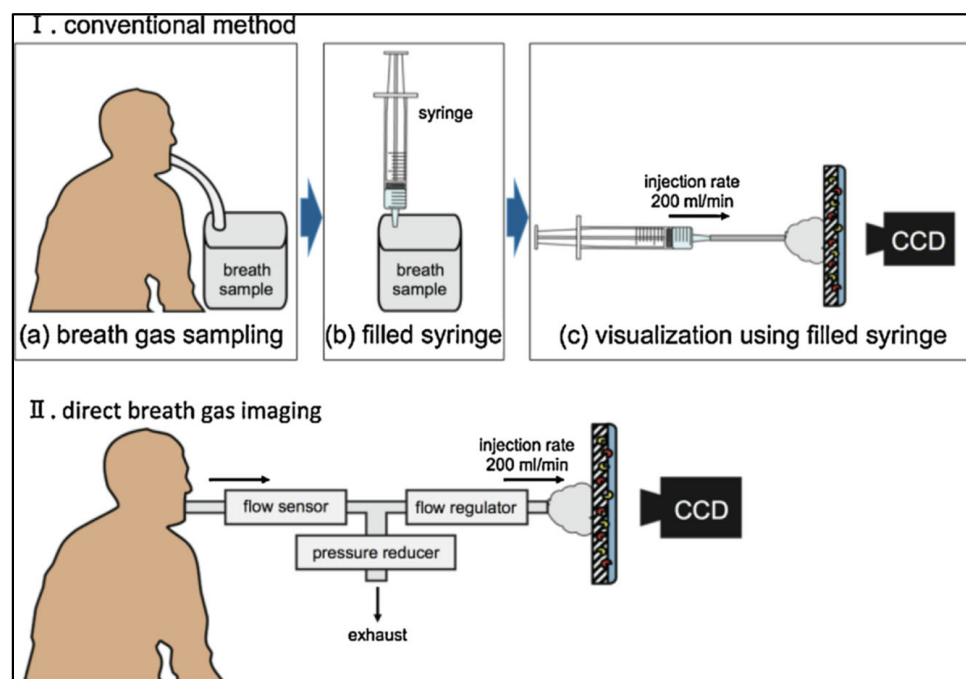
Figure 6. Sampling methods for breath analysis (**I**) using a breath sampling bag and syringe. (**II**) Exhaust breath flow control system for direct breath analysis without a gas sampling bag [145].

3. Sensors for Volatolome Analysis: Principles & Mechanism

3.1. Types of Sensors

Sensors can convert a variation in their environment into an interpretable signal; they belong to three categories depending on the quantity they measure: physical (temperature, pressure, magnetic field, and resistance), chemical (reversible and irreversible interactions, concentration, pH), and biological (interactions and expression of an activity) [146]. Chemical sensors that are of particular interest for the analysis of volatiles in breath to diagnose diseases can produce optical, frequency, electrochemical, and chemo-resistive signals.

Optical Sensors can use fluorescent dyes embedded in the polymer matrix which cause spectral bands to change when the macromolecules interact with the vapour molecules [147,148]. Frequency sensors are called quartz crystal microbalances (QCM) or surface acoustic waves (SAW). The resonance frequency of their quartz crystal expressed by SAUERBREY's equation [149] is shifted when gas molecules are absorbed on their surface, due to the change in mass. This technique can be selective to analytes by changing the crystal coating nature, polymer or metal oxide. Contrarily to QCM, SAW sensors analyse the surface waves generate along the surface instead of in the bulk [150–153].

Optoelectronic Sensors use surface plasmon resonance imaging (SPRI); they can be assembled into arrays to make an e-nose. They consist of a prism coated with a thin gold layer functionalised with a series of biomimetic peptides and organic molecules such as thiols with diverse physicochemical properties (hydrophobic, hydrophilic, charged, neutral, etc.) using a non-contact microspotting robot. A collimated beam with a wavelength of 632 nm from a LED is polarized and sent towards the functionalized gold surface through the prism to illuminate the entire microarray. Surface plasmon resonance causes a progressive variation in the reflectivity (%R) when VOCs present in the dielectric medium in the gas phase interact with the sensing material on the microarray [154].

Electrochemical Sensors have potentiometric (potential difference between electrodes), amperometric (intensity variation), or impedancemetric (complex resistance variation) typical output signals. Generally, the sensitivity relies on the interaction between the

electrode and analysed gas and the selectivity results are from the nature of the electrodes and eventually the membranes [155,156].

Chemo-Resistive Sensors have semiconductor transducers which resistance changes upon adsorption of analyte molecules. One interesting feature for applications is that their sensitivity can be easily modified by changing their nature or composition [157–159]. The semiconductor transducers can be made of metal oxide, intrinsically conducting polymer (ICP), and conducting polymer nanocomposites (CPC). The variation in their chemoresistive response can be used directly or indirectly in field-effect transistors (FET) [160]. But whatever the design, their principle is based on the interaction of vapor molecules with the adsorption sites of the transducer's surface that will change its resistivity [161].

3.2. Chemo-Resistive Sensors

Metal Oxide Sensors (MOSs): n-type transducers such as zinc oxide, tin oxide, titanium dioxide or iron(III) oxide can interact with reducing vapours like hydrogen, methane, carbon monoxide, ethylene, or hydrogen sulphide whereas p-type transducers such as nickel oxide and cobalt oxide react with oxidizing gases like oxygen, nitric oxide, or chlorine [162]. To look for synergistic effects, more recent works focus on composite MOSs such as SnO_2-ZnO, Fe_2O_3-ZnO, and ZnO-CuO [163]. Metal oxide particles use substrates such as alumina, glass, and ceramics on which they are deposited by screen printing [164], spin coating [165], or vapor deposition [166]. The connection electrodes are made of gold or platinum with the same process.

One drawback of MOSs is that most of them need to work at temperatures as high as 200–500 °C although some can operate at lower temperatures when hybridized with carbon nanotubes for the detection of NO_2 [167]. Shobana et al. [168] reviewed the use of MOS hybrid sensors to detect gases and VOC biomarkers. Hybrids of palladium tin oxide and pristine graphene (Pd-SnO_2/PRGO) transducers were found to discriminate CO from NH_3, ethanol, acetone, and CO in the range of several hundred ppm.

Additionally, moisture was found to divide by two the sensitivity of Sm_2O_3-doped SnO_2 when relative humidity was raised from 0 to 33% [163]. Moreover, the SiO_2 transducer's thickness that varied from 14 to 74 nm resulted in responses to 2% hydrogen decreasing from 84% to 32%, respectively [169]. Nevertheless, operating gold nanoparticles functionalized with WO_3/SnO_2 nanofiber at 105 °C gave a response of 79.6% for 0.5 ppm of acetone at 150 °C and 90% relative humidity [168].

Another disadvantage of metal oxide sensors is that they can be poisoned by irreversible interactions with some sulphur-containing gases for instance [170]. Despite their wide use in the design of e-nose and their well-controlled fabrication in cleanrooms, the above-mentioned limitations of MOSs related to an inherent dependency of sensitivity to the active layers' thickness, humidity and operating temperature, and a selectivity hard to adjust, have pushed researchers to investigate the development of alternative organic transducers.

Conducting polymer nanocomposites (CPCs) have been widely used to make transducers of environmental parameters, such as temperature, pressure, strain or volatile content [171]. The versatility of CPC transducers allows the design of sensors that can be flexible [172] or integrable [173], and their fabrication does not require cleanrooms as MOSs. Their principle of CPC vapour sensors is much simpler as they only need an insulating substrate on which electrodes are deposited (Figure 7).
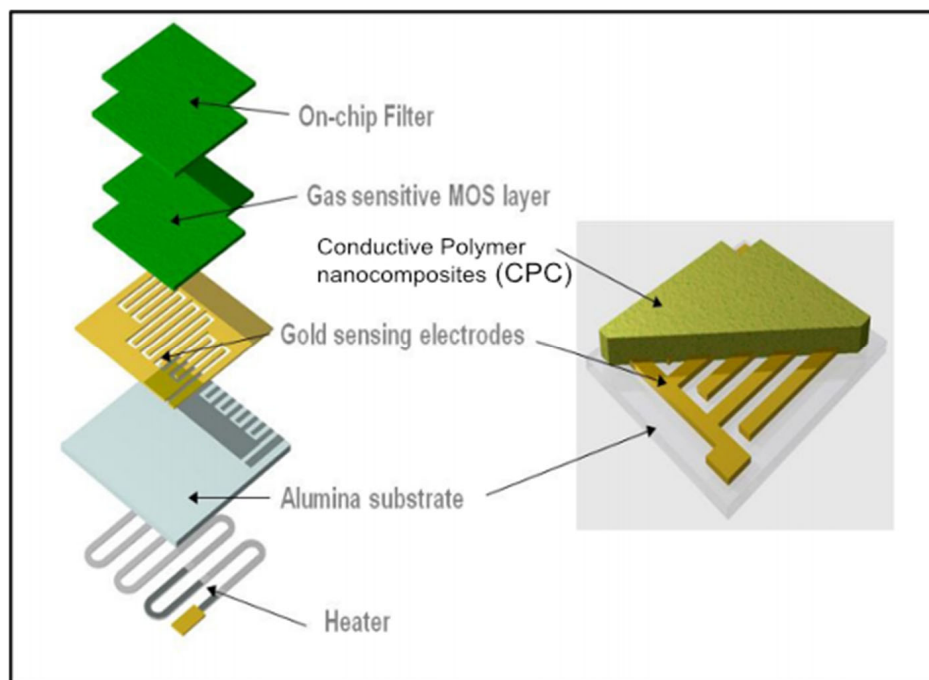
Figure 7. Comparison in the design of metal oxide sensors (**left**) with conductive polymer nanocomposite sensors (**right**) [170,171].

They can be synthesised at room temperature by dispersing different types of conducting fillers such as carbon or metal nanotubes, nanorods, nanobelts or nanowires in a variety of polymer matrices that are either thermoplastic or thermoset, further spayed or printed [174]. Eventually the formulation of CPCs can be eco-designed to decrease their impact on the environment by using green carbon nano-onions from exhaust soots [175] or biobased polymers [176]. However, carbon nanotubes, among all allotropes, have been most extensively used to develop vapour sensors thanks to their exceptional electrical (ability to transfer electrons) and morphological (interconnectivity, shape factor) properties [177]. They also have excellent stability [178] that makes them very attractive for the fabrication of new components in electronic devices like chemical sensors and biosensors.

CNTs were first discovered by Lukyanovich et al. [179] and further popularized by Iijima in 1991 [180]. Since then, many studies have evidenced their unique surface and mechanical, electrical, and optical properties [181]. CNTs are members of the fullerene family and can be found as single-walled (SWCNT), few-walled (FWCNT) or multi-walled (MWCNT). SWCNTs are like seamless cylinders of one atomic layer of graphene sheet which has a diameter of nanometres and a length of up to 100 microns (Figure 8). MWCNTs are made of concentric cylinders of graphene tubes [182]. Carbon nanotubes have highly anisotropic dielectric properties as CNTs can possess a high electrical current with the least heating effect [183]. CNTs are mostly prepared by the following three methods: arc discharge, laser ablation technique, and chemical vapor deposition (CVD). High-quality SWCNTs can also be obtained by using an appropriately optimized catalyst system [184,185].
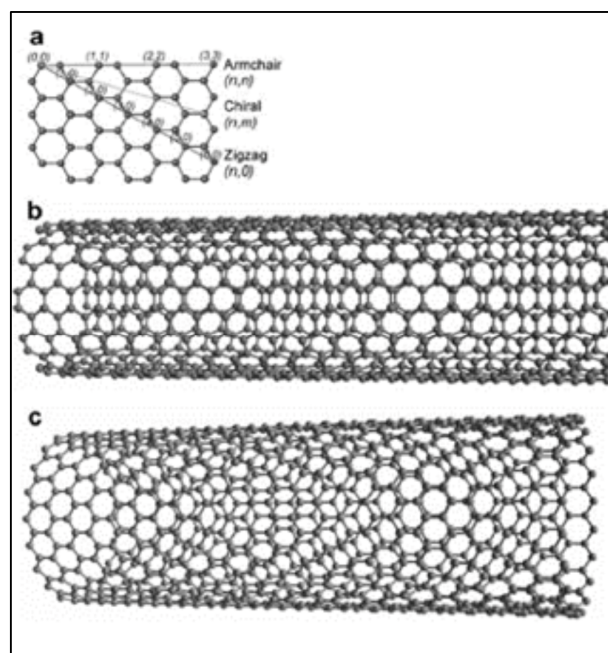
Figure 8. (**a**) The wrapping vector of a graphene sheet defines the structure (chirality) of a carbon nanotube. Examples of (**b**) "armchair" and (**c**) "zigzag" SWCNT [186].

Pristine CNT do not exhibit high selectivity towards solvent vapours and they therefore have a limited scope in their pure form. But by altering the chemical functionalization of CNTs, some selectivity can be generated in their behaviour [187,188]. Sin et al. showed that treating CNTs with concentrate acid (3:1 of H_2SO_4 and HNO_3) could generate some acid groups on the surface (Figure 9). These modified CNTs showed a good response towards alcohol due to the increased dipole–dipole interaction between the CNT surface and polar molecules. Functionalized CNTs showed an increased sensitivity from 0.9 to 9.6% [189].
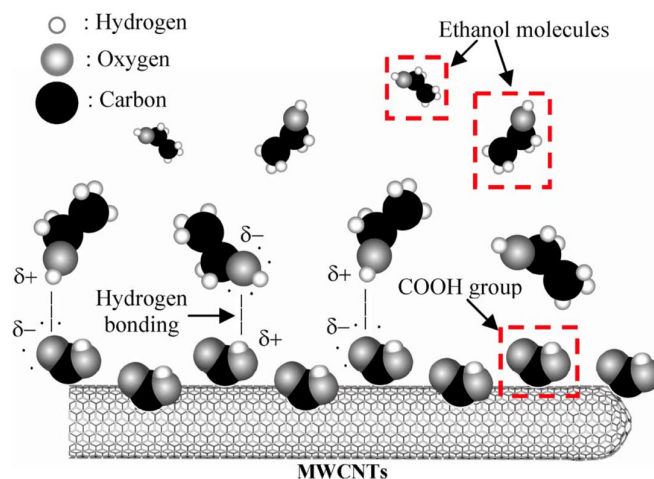
Figure 9. Schematic diagram of the chemically functionalized carbon nanotubes with COOH groups and mechanism for alcohol vapour detection using f-CNT sensors [190].

An oligomer of poly(ε-caprolactone) grafted from a CNT was found to enhance the sensitivity of the resulting CPC to toluene, tetrahydrofuran, and chloroform [177], whereas polyhedral oligomeric silsesquioxanes (POSS) covalently bonded to the surface of functionalized CNTs have proved to boost their selectivity to cyclohexane and pentane

vapours or to acetone, butanone, propanol, and toluene when functionalized, respectively, with iso-octyl and phenyl groups [191].

Other modifications on CNT have been carried out to increase their sensitivity towards hydrogen (H_2). H_2 sensing is very important because of safety and handling issues, but due to the poor binding energy of CNT, only Pt- and Pd-functionalized CNT were sensitive toward H_2 [192,193].

When CPC-based sensors are exposed to vapour molecules, they partially swell the macromolecules coating the carbon nanotubes junctions, which results in a tiny volume expansion (some nm^3) that triggers multiple nano-disconnections in the percolated conducting architecture, increasing quantum tunnelling conduction. The macroscopic effect of this phenomenon is an exponential variation of resistance of the CPC transducer with the average inter-tubes' distance [194]. Such sensors can thus be named quantum resistive vapour sensors (vQRS) [195].

Nanofoils of reduced graphene oxide (rGO) and their hybrids with silver nanoparticles (AgNP) [196], Cu_2O nanocrystals [197], ferrite (Fe_3O_4) [198], fullerene (C_{60}) [199], metal oxides (MOSs) [200], Mxene [201] or metal organic frameworks (MOFs) [202], eventually in association with polymer matrices such as poly(methyl methacrylate) PMMA [203], poly(aniline) PANI [204], poly(3,4-ethylenedioxythiophene) (PEDOT) [205], or poly(pyrrole) PPY [206] are also emerging for vapour sensing. Graphene has the advantages to exhibit abundant adsorption sites and high-charge mobility which can lead to higher sensitivity provided that its assembly leads to an easily disconnectable conducting architecture, otherwise the superimposition of layers will decrease the amplitude of the chemo-resistive response [207].

3.3. Developments in Volatile Organic Compounds' Sensors

Several research groups have tried to create sensors with increased performance as well as different architectural designs. These researchers are coming up with various strategies and designs to improve the performance of VOC sensors and bring sensing technology closer to real-time applications. In 1992, Gardner et al. suggested e-noses could be further used to diagnose potential health risks by analysing volatiles in human breath. In 2000, this research group investigated multiple applications of e-noses and VOC sensors to determine their potential use within industries of food, beverage, meat, tobacco, and perfume. Further, they have designed a metal oxide-based e-nose (based on Fox 2000 Alpha MOS SA) that has been studied for its capacity to mimic the olfactory capabilities of the human nose and discern different types of odours [208,209]. In addition, N. Lewis et al. studied the detection of VOCs using carbon-based sensors [208,209]. The researchers employed carbon nanoparticles as a conducting filler in non-polymeric organic substances such as lauric acid, propyl gallate, and dioctyl phthalate to fabricate a sprayed film. They measured the change in resistance of the sensors upon the vapor molecules' sorption. Then, they employed the Fisher Linear Discriminant algorithm to evaluate the performance of the sensors which appeared to have a limited sensitivity to the studied volatiles. Moreover, the analytical technique employed was found to be complicated [210].

In their work, Di Natale et al. employed vapour sensors as a diagnostic tool to analyse the exhaled breath of lung cancer patients. The authors used quartz crystal microbalance (QCM) combined with an array of metalloporphyrin-coated sensors. They demonstrated that these sensors possessed the capability to analyse the volatile biomarkers typically associated with lung cancer. Furthermore, they were able to effectively differentiate between cancer patients and control subjects from the analysis of breath samples' patterns [152,211,212].

Persaud et al. developed a simulation software for conducting virtual e-nose experimentation and a software tool to analyse data. They have used seventeen polymer sensors with analytes at different concentrations and used their profiles as reference data for the simulation software. Using this software, an e-nose can be simulated with varying types or numbers of sensors for the analysis of different solvents. This array of virtual sensors can be controlled in terms of noise level, drift, and affinity towards analytes. The data generated by the simulation can be easily analysed by the software tools associated with it. They studied and developed a very rapid and computer-based technique for VOC analysis which is available for other researchers in this field without any cost [213].

Haick et al. have focused on the analysis of biomarkers for lung cancer, including their development within the human body and the corresponding patterns observed in breath samples [214]. The authors used metal nanoparticles like gold to fabricate sensors in combination with quartz crystal microbalance and GC–MS technique to analyse the VOC pattern in lung cancer [215]. In their study, they proposed specific poly (cyclic aromatic hydrocarbon) (PAH) derivatives to sense the nonpolar VOCs. Using metal oxide sensors, they identified forty-two VOCs in a cancerous breath [216]. Despite interesting results, metal oxide-based sensors still have some drawbacks in comparison to polymer sensors as they require high operating temperatures, they damage in the presence of moisture, and they require costly electrodes such as Au or Pt. Accounting for such drawbacks, the researchers have prepared monolayer-capped gold nanoparticles and chemically functionalized single-walled CNT (with dodecane thiol and chlorobenzene methanethiol) in the year 2016 to detect seventeen different diseases including lung, colorectal, ovarian, and kidney cancers, among others, from patients' breath. A total of fifty-nine different sensing parameters were calculated using the data collected from the sensors to derive the breath print associated with these specific disorders. The researchers demonstrated that each disease possesses a distinct breath print, as depicted in Figure 10. The proposed e-nose finally showed 86% accuracy in recognizing the disease pattern in blind tests of various breath samples [217].
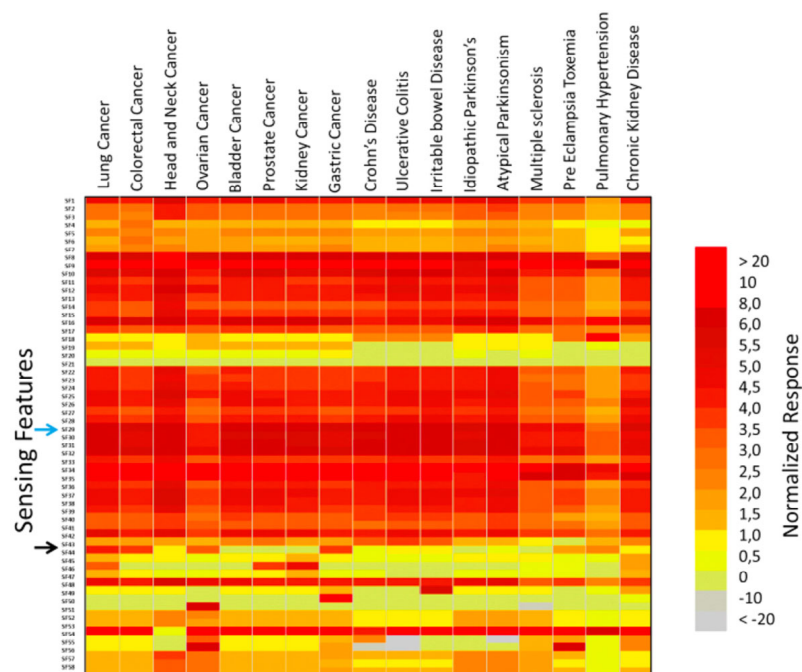

Figure 10. Breath print of various diseases obtained by a nanoarray with 86% accuracy in disease recognition [217].

Another approach to guide developments of e-noses is to be inspired by nature. Biomimicry, although difficult to implement in the case of mammal olfaction due to the complexity of each step in odour identification, can lead innovations. Hou et al. in their review [218] report different initiatives in this way. For example, combining generalist and specialist (modified by proteins) transducers, as is the case for human olfactory receptors, can improve selectivity [219]. Or mimicking the highly specific surface of receptors in moth antennae can act as a preconcentrator [220]. Olfaction data treatment in the brain can also inspire: neurons use time descriptors and it was found that this parameter could improve the classification with PCA [154], whereas the first two stages of the olfactory pathway (distributed coding with olfactory receptor neurons and chemotopic convergence onto glomerular units) can be integrated into a neuromorphic model that is able to significantly enhance the signal-to-noise ratio of chemo-resistive responses from sensors array [221].

3.4. Nanotoxicity

The field of nanotechnology is currently seeing significant growth, paralleled by an increasing demand for nanomaterials and nanoproducts. Consequently, there has been a rise in the level of exposure to these compounds, necessitating the examination of their impacts on both the environment and human health [222]. Nanotoxicity is contingent upon various factors, including the inherent characteristics of the particles, such as their size, shape, and dimensions, as well as the duration of exposure. The primary route of toxicity for humans in relation to these nanocompounds is through skin absorption, whereas inhalation is considered a secondary pathway. Research has demonstrated that nanoproducts, such as CNTs, can penetrate deep into the lungs when individuals are exposed to them for extended periods. Depending on the concentrations of nanoparticles, a prolonged exposure can result in the degradation of tracheal tissues and membranes [223,224]. The nanotubes can also be transferred into the blood from the lungs, thus potentially affecting the heart and other body parts [225]. The fibrous nature of CNTs, often compared with asbestos although their shape factors are very different, could cause mesothelioma upon long exposure [226]. Nanotubes are also suspected to be carcinogenic and able to affect DNA structure and lead to unwanted mutations [227]. In addition to this, MWCNTs can cause acute pulmonary toxicity, subpleural fibrosis, immune suppression, etc. The toxicity of CNTs also depends on their level of impurity, chemical treatment, physical form, surface chemistry, degree of aggregation, etc. [228]. For example, in the case of in vivo toxicity effects, MWCNTs are found to be more toxic than SWCNTs. Furthermore, it can also be studied that well-dispersed CNTs have less toxicity compared to agglomerated CNTs.

In the case of in vitro studies, the researchers have studied the interaction between CNTs and cells, and it was found that functionalized CNTs have less cellular toxicity. This study suggests that the purification process could enhance their biocompatibility because macrophages (which remove particulate from tissues) can digest 7.3 μg·cm^{-3} of SWCNT without any toxicity. The effects of toxicity on other living organisms have also been studied since contamination has delayed the hatching of zebrafish embryos, subsequently causing lower survival rates among second-generation breeds. Further, these CNT can potentially accumulate within the gastrointestinal tract of primary consumers in a food chain, thereafter, undergoing gradual translocation to higher trophic levels. Short and sharp CNTs in the shape of nanodarts can possess antibacterial capabilities due to their ability to disrupt the cell walls of microorganisms. However, the mechanism of CNT toxicity has not been cleared yet and the correlation between in vivo and in vitro toxicity effects is not established, thus requiring further efforts in exploring the core of nanotoxicology [229].

Besides nanotubes, graphene nanoplates (GNP) and their derivatives are also emerging as very useful nanomaterials in different applications, for instance, biosensing, drug

delivery, antibacterial materials, and tissue engineering. However, GNP also have potential toxic effects on living organisms during long exposure. These GNP can enter the body during breathing, via the oral route, and by injection which can damage the body tissues severely as shown in Figure 11. For example, graphene nano-aerosol can be inhaled resulting in a very high amount of graphene deposited in the lung trachea. This can lead to granulomas, lung fibrosis, and tissue decay of the affected person. Furthermore, it was suggested that GNPs could also penetrate inside the body through skin tissues and can create skin toxicity [230]. There are other toxicities such as the cytotoxicity of graphene depending on the particle size. For example, nanoparticles smaller than 100 nm can penetrate the cell membrane, then particles less than 40 nm can penetrate the cell nucleus, and finally very small particles less than 35 nm travel across the blood–brain barriers [231]. Moreover, GNP toxicity also depends on the concentration. Some experiments showed that a 0.25 mg dose of graphene oxide in mice did not show any toxic signs but when the dose was higher than 0.4 mg, it led to fatal effects [232].
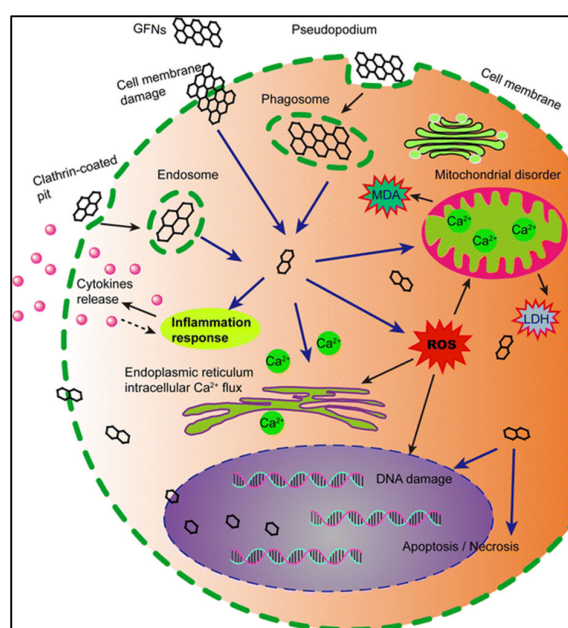
Figure 11. Schematic showing the mechanisms of graphene cytotoxicity and its adverse effects on cells (cell membrane damage, inflammation, DNA damage, and mitochondrial disorders) [230].

However, the likelihood of experiencing hazardous consequences from vapor sensing is minimal due to the effective encapsulation of nanoparticles within the matrix, preventing their easy release. Additionally, the probability of direct contact of CNTs between users and sensors is minimal. This implies that the utilization of these sensors does not pose any adverse impacts on users in terms of toxicity, thus broadening the scope for their practical applications in real time.

4. Electronic Noses (E-Nose)

4.1. Working Principles

The e-nose was originally designed to emulate the operational principles of the human olfactory system. The human nose is a naturally developed complex sensing array. The nasal epithelium is comprised of a multitude of receptor cells that possess the ability to detect a diverse array of chemicals and odours. The olfactory signals are transmitted to brain cells and afterwards, they are analysed by the brain. It is worth noting that human nose receptor cells can detect over 10,000 different chemical vapours. For this function, the

human nose contains around 1000 smell receptor genes in cells as well as a complex neural network to process it [233]. Therefore, the human nose is very efficient in odour analysis. Similarly, the e-nose is thus based on the natural nose's working mechanism as depicted in Figure 12.
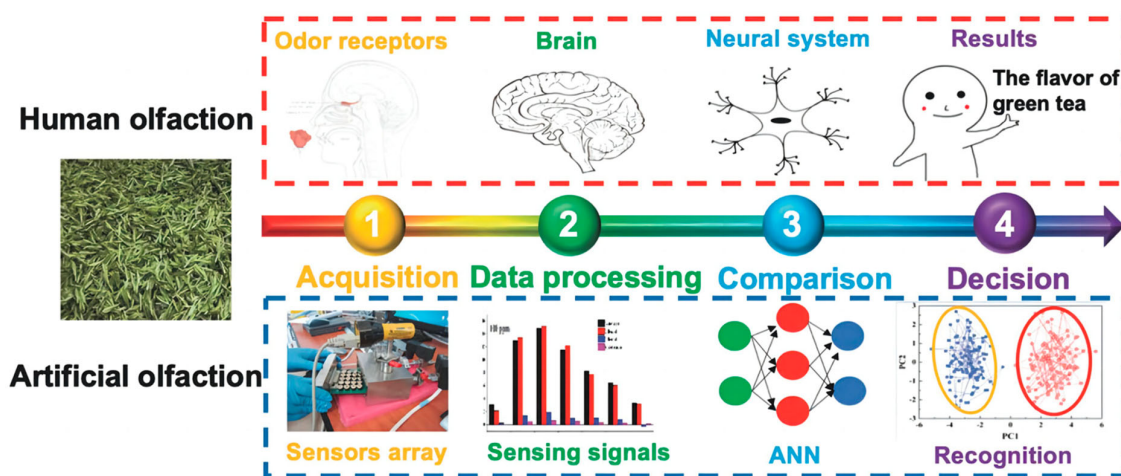
Figure 12. Comparison of the human nose with an artificial nose [234].

This principle can be applied to disease detection using different types of artificial receptors, i.e., chemical vapor sensors' array [161]. The array is the combination of several and/or different types of sensors that can detect various types of VOCs (being specific or non-specific). This sensor array or so-called electronic nose (e-nose) can be used to analyse complex mixtures of VOC and to generate the corresponding pattern.

Regarding medical applications, human breath, which contains a complex system of VOCs, can be classified into different breath prints in relation to an individual's health status. To analyse the breath print obtained from the e-nose, it is necessary to employ proper mathematical models and implement a programmed neural network, as shown in Figure 13, to distinguish between the healthy and diseased breath prints [235–237].
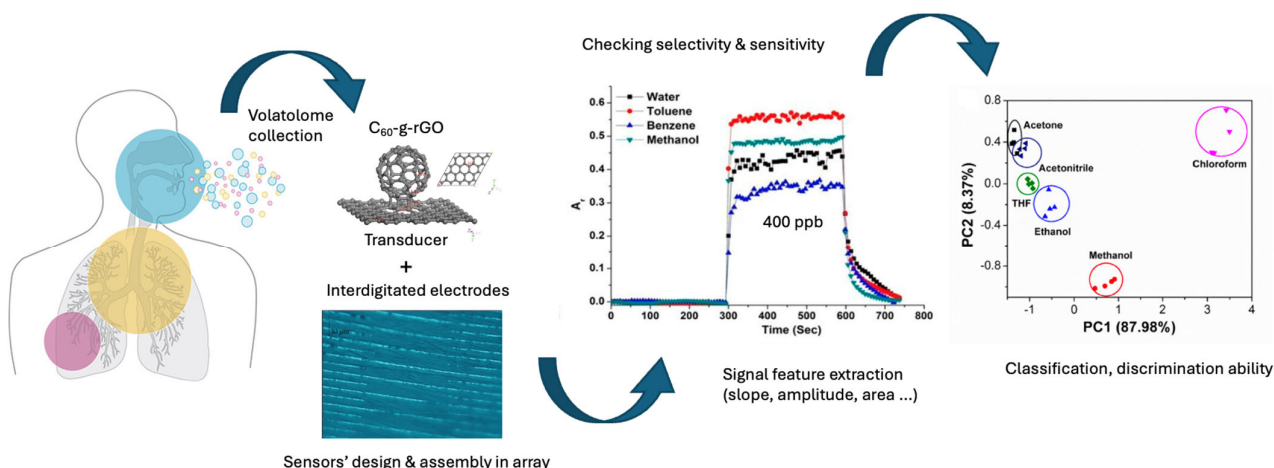
Figure 13. Different steps involved in e-nose working and pattern recognition [202,238–240].

The main components of an e-nose system are a sample inlet mechanism, sensor array, and signal measuring and recording unit [241]. When breath samples are introduced inside the e-nose, sensors start interacting with different components (physically or chemically based on the chemical nature of VOCs) of the breath. This interaction leads to signal generation [208,242]. These electrical signals have been recorded by the software for the

purpose of analysis. Konvalina et al. [243] have described the process of breath sensing using chemical sensors. The protocol of the process has been clearly described in Figure 14. The process of analysis of data and prediction from breath patterns involves the utilization of feature extraction and pattern recognition algorithms. In the case of breath testing, the collecting of samples is seen as a crucial step that requires highly controlled measures to prevent any loss of valuable VOC.
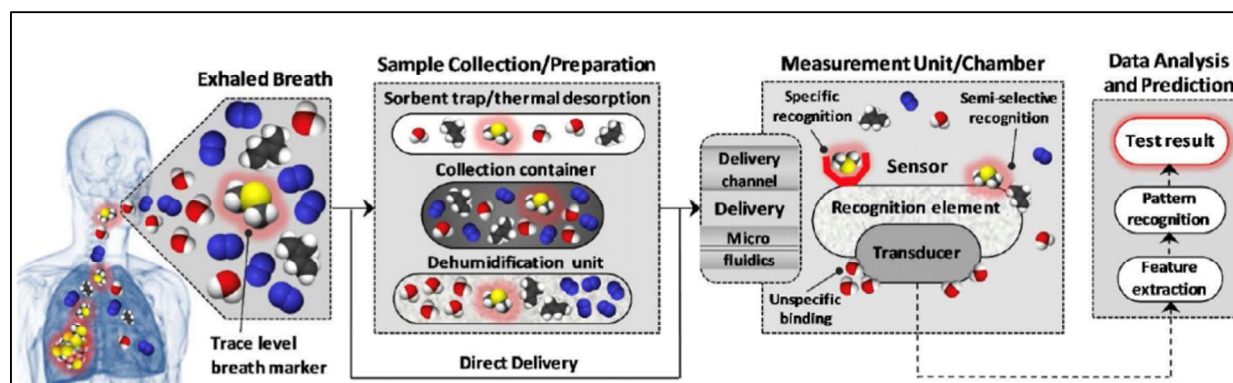
Figure 14. Important steps in e-nose application: sample collection to avoid loss of useful VOCs [243].

To distinguish between healthy and diseased volatile samples is complex as the diseased state is not characterized by a single VOC but instead, olfactive prints composed of several vapours not all identified. The e-nose must detect this change in the volatiles' profile durably and associate a print to a health condition with enough accuracy, meaning that a proper learning has to be done [209]. However, an e-nose appears to be an alternative full of promises for clinical diagnosis and disease detection since it is non-intrusive, eventually portable, easy to operate and to install, rapid, and does not require specialization, i.e., a very promising prospect for medical diagnostics if data are collected in large amounts with suitable algorithms.

4.2. Data Treatments

Data collection is the first step of a diagnosis based on an e-nose system, before result interpretations and data analysis. The software records the electrical signals characteristic of interactions between sensors and volatiles. Special care must be taken to the data recording system and transducers that could otherwise alter results. After feature extraction from a given data set, it is necessary to reduce dimensions from the multidimensional data collected from the electronic nose (e-nose), which poses challenges in its interpretation due to its original complexity. Two types of features are extracted from the data generated by the e-nose, some with physical significance such as signal amplitude or normalized sensor response, and others called mapping features. The latter are obtained from temporal data [244]. All these features are collectively required for data interpretation. From all these features, the most effective features having the least number of errors are selected for the pattern recognition algorithm. This process is termed feature extraction. Pattern recognition is the final step in the e-nose data analysis to predict the status of the breath for different diseases. The pattern recognition techniques are statistical methods such as principal component analysis (PCA), analysis of variance (ANOVA), linear discriminant analysis (LDA), K-means, hierarchical cluster analysis (HCA) [245], principal component regeneration (PCR), etc. [246,247]. These methods reduce the complexity of the e-nose data and generate very convenient patterns. Artificial neural networks (ANN) are not commonly used for e-nose data interpretations, but they have a very intuitive approach to pattern

recognition. ANN include multilayer perceptron (MLP), self-organizing map (SOM), radial-based function networks (RBF), and linear vector quantization (LVQ) [244,248].

PCA is also called singular value decomposition (SVD). PCA is an unsupervised classification method. The results of PCA can be plotted in 2D or 3D to understand the vapor-sensing discrimination for different VOC groups. The feature points obtained by PCA treatment are not correlated to each other. These points on the map are linear combinations of an original data set of e-nose sensors. This method is used to reduce the dimensions of data with minimum loss in the information as shown in Figure 15 where the different families of vapours appear well separated. PCA is used to identify different chemical groups of VOC. It is a very simple and fast method, but some information associated with the non-linear correlation of the original data can be lost.
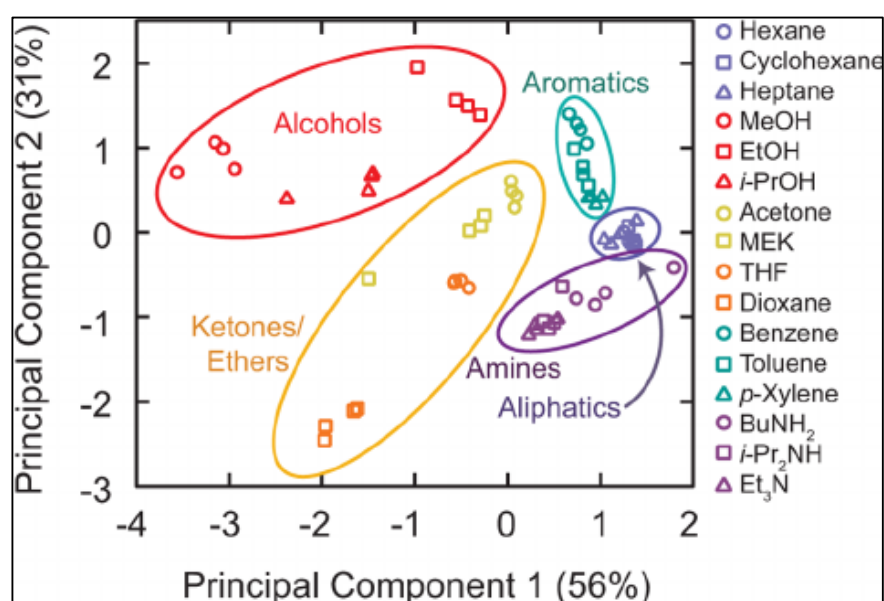
Figure 15. Identification of different chemical groups using the PCA algorithm (plotted in a 2D map) [249].

LDA is a type of discriminant function analysis (DFA) method. These methods were first used by Fisher [250,251]. This is a supervised feature extraction technique. It also has a linear correlation with original data points. The supervised linear correlation can minimize the scattering of data points for the same group. As shown in Figure 16, LDA curves are obtained by two separate measurements for five different types of juices and points for a particular group are well clustered.
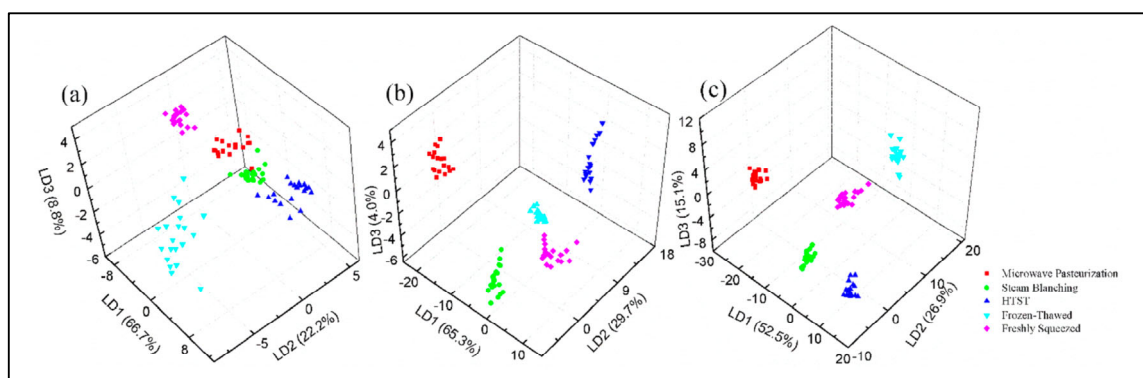
Figure 16. LDA discrimination of five different strawberry juices. (**a**) E-nose measurement, (**b**) e-tongue measurement, and (**c**) combining both e-nose data and e-tongue data [252].

An ANN is based on a non-linear correlated variable mapping technique. It has some advantages over usual feature extraction techniques, as an ANN involves a network topology that has a learning algorithm. The utilization of a trained neural network holds significant importance in e-nose data analysis and pattern recognition. Multi-layer perceptrons (MLPs) are the most used form of ANN. It has layers of neurons with each neural layer for input and output. Other layers are called hidden neural layers and they are connected to the input and output layers as shown in Figure 17. Furthermore, the backpropagation algorithm has been widely employed for training ANN [253,254]. The training of ANN enhances its efficiency for feature extraction. ANN are a predictive method that can classify unknown odours or vapours while PCA or LDA are only exploratory methods that can create groups from multi-dimensional data for easy understanding [255].
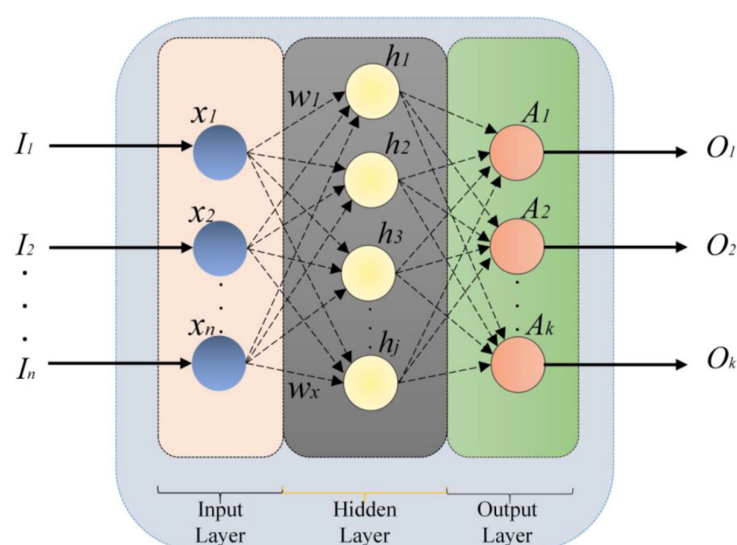
Figure 17. A three-layer MLP neural network [256].

4.3. Artificial Neural Networking

In recent years, major progress has been achieved in the food, agriculture, health, and other sectors due to the rapid development of e-nose sensors supported by artificial neural networks. In the e-nose system, it is important to find a suitable algorithm that can process the response from sensors under exposure to different VOC. The selection of an algorithm able to make pattern recognition is a key point [257]. It must fit data distribution to enhance the sensors' response and supress redundancy to improve pattern accuracy which is a major challenge [258]. Owing to such criteria, artificial neural networks (ANN) can be an interesting alternative to conventional computer algorithms.

An ANN is composed of interconnected networks that operate in parallel to find a solution similar to the way a human brain processes information. Every neural flow of the ANN contains three different layers that are input, hidden, and output layers [259]. The input layer in the ANN is fed with a library of data files in the computer or the response of the sensors in real-time, while the data are processed in the neural networks. Once the data are processed in the neurons, it forwards these data to the output layer. These layers deliver these data back to the user through a secondary control system. The hidden layer in an ANN consists of neurons that execute functions on the input data. However, the data processing completely depends on the way these neurons are interconnected. In general, the user can establish the neural network by modifying neural connections, which implies that depending on the user's requirement, the user either adds or deletes neurons [257,259].

Furthermore, this established neural network can be trained using one of two approaches: (1) unsupervised training and (2) supervised training. In the supervised training

approach, the user must provide the desired output to the ANN by ranking the performance of the ANN. On the other hand, the system only feeds the neural network with the library of data files without giving any further instructions and the system adapts itself to find the desired output in the unsupervised training approach. However, the unsupervised training approach has not yet obtained similar outcomes when compared to the supervised training approach. The sensor array can develop the neural network depending on two different approaches to differentiate the VOCs. In the first approach, the network can gather the responses from sensor arrays for each specific VOC. In another approach, the network can gather the responses from sensor arrays for a group of various VOCs [257,259].

Schroeder et al. used a chemo-resistive sensor array to classify the different food samples including edible oil, liquor, and cheese. The author fed the input layer directly with the responses of the sensor. The author suggested that the samples were differentiated based on the initial conductance and the recovery period of the ANN. The designed ANN could differentiate the food samples with an accuracy of 73% for the edible oil, 78% for liquor, and 91% for cheese, indicating the system's potential for future applications [260].

Pavlou et al. developed an e-nose and an intelligent odour-recognition system. The authors successfully discriminated *Helicobacter pylori* from other bacterial gastroesophageal isolates by extracting fifty-six normalised features from responses of fourteen sensors. These variables were analysed by a three-layer back-propagation ANN. They obtained an ANN prediction rate of 98% and 37.7% of all test data were recognised correctly [76].

Aguilera et al. studied the aroma of young white, young red and aged red wine samples using a multisensory array system. They classified these samples using independent component analysis combined with an ANN. They obtained classification success rates of 94%, 84%, 82% for young white, young red, aged red wines, respectively [261].

Leggieri et al. developed an e-nose combined with an ANN for the analysis of mycotoxins such as aflatoxin B1 and fumonisin in maize. The research group has collected data over 5 years for the analysis of mycotoxins and developed ANNs for the assessment of aflatoxin B1 and fumonisin. However, the e-nose supported with statistical analysis demonstrated an accuracy of 80%, whereas ANNs exhibited an accuracy of 77.36% for aflatoxin B1 and 78.26% for fumonisin [262].

Tan et al. determined the degree of roasting in cocoa beans using an e-nose supported with a three-layer backpropagation ANN. The author categorized cocoa beans as unroasted, lightly roasted, and dark roasted using a nine-sensor array system. The responses from the sensors were analysed using an ANN and their accuracy was compared with GC–MS data. Overall, the e-nose supported with an ANN exhibited an accuracy of 94.4%, whereas GC–MS data demonstrated an accuracy of 95.8%. Both models had 100% prediction for unroasted and roasted samples [263].

Panigrahi et al. developed an e-nose containing 32 Cyranose-320TM conducting polymer-based sensor arrays for the analysis of spoiled beef meat. They collected VOC samples from the headspace of fresh beef meat stored at 4 °C and 10 °C. The responses obtained from the e-nose were processed with the radial basis function neural networks for classification of spoiled and unspoiled beef meat samples. These ANNs successfully classified the spoiled and unspoiled meat with an accuracy of 100% [264].

D. Zhang et al. developed Tin dioxide (SnO_2) nanospheres decorated with a graphene sensor array for the detection of formaldehyde and copper oxide (CuO) nanoflowers decorated with a graphene-based sensor array for the detection of ammonia gas. The responses from the sensor systems were analysed with a backpropagation (BP) neural network. They reported that an integration of a nanostructured sensor array and a backpropagation (BP) neural network model can recognize multiple gas species and accurately estimate their concentration [265].

Aghilinategh et al. developed an e-nose to determine the quality of berries and classify them based on maturity into five different levels. Statistical methods such as PCA and LDA were used to analyse the responses of the sensor. However, PCA and LDA exhibited lower discrimination rates to classify the berries. On the other hand, ANN were applied to the sensor array responses and demonstrated a discrimination rate of 100% [266].

Zakaria et al. used a multi-modality sensor array containing thirty-two sensors supported with probabilistic neural networks to determine the adulteration of pure honey. In their study, the group used eighteen different sets of samples to differentiate the pure honey from adulterated honey and sugar syrup. The sensor system was able to classify the samples with different compositions with the highest accuracy of 94.44% [267].

Machado et al. analysed the exhaled breath composition of fourteen bronchial cancer patients using the Cyranose 320. Support vector machine (SVM) analysis was applied on the responses from the sensor array and it exhibited a specificity of 91.9% and accuracy of 71.4% for detection of cancer. Furthermore, the sensing system was able to discriminate olfactory characteristics of control subjects of non-small cell lung cancer, chronic obstructive pulmonary disease, and healthy patients [268].

In relation with this study, Chen et al. diagnosed lung cancer using a virtual gas sensors array of surface acoustic waves. The output responses of these sensors were analysed by an image recognition method combined with an ANN. This sensor system can detect the 11 different biomarkers related to lung cancer and successfully diagnosed these biomarkers for real-time application in the hospital [269].

Nurputra et al. developed a low-cost and portable e-nose (i.e., GeNose C19) based on a sensor array which identified COVID-19 through expiratory breath fingerprinting. The research group assessed breath profiling tests including a total of 615 breath samples. The testing profiles were analysed by four different machine learning algorithms such as deep neural network, stacked multilayer perceptron, linear discriminant analysis, and support vector machine. These methods have demonstrated high performance with a system detection accuracy range of 88–95%, a sensitivity range of 86–94%, and a specificity range of 88–95%. The results suggested that this sensing system is highly effective in detecting COVID-19 [270].

Like this sensing system, Kwiatkowski et al. prepared an electronic setup comprising of commercial VOC sensors for the detection of COVID-19. Receiver-operating characteristic patterns were generated for a total of fifty samples, in which thirty-three samples were collected from infected patients. The responses of the sensor system were analysed using four detection algorithms including a multi-layer perceptron algorithm (Neural Network widget), random forest, k-nearest neighbours' algorithm, and support vector machine (SVM) algorithm and the highest detection accuracy of 84% was exhibited [271].

The above research shows the great potential of e-noses in diagnostics in many fields of research from the analysis of volatile organic compounds, especially those emitted by the human body. According to the literature, the use of both commercial and self-developed sensing systems is majorly increasing in clinical medicine fields and commercial industries in recent years [272]. Furthermore, the association of e-noses with ANN-based algorithms will provide great prospects for their wide range of potential applications in health care, food industries and commercial sectors.

5. Performances of E-Nose in Biomarkers' Detection

5.1. Sensors' Characteristics

Classically, the vapor transducers selected to be assembled into an e-nose can be defined by various characteristic parameters that condition their performances. To improve them, it is useful to recall their definitions in Table 2 [273].

Table 2. List of sensors' characteristics.

Characteristics	Definition
Sensitivity	Change in the measured signal per unit of the vapor concentration and it can be calculated from the slope of response vs. concentration.
Selectivity	The response towards a specific solvent or family of solvents.
Stability	Ability of sensors to give reproducible results including sensitivity, selectivity, and response over a period.
Detection limit	The lowest limit of vapor conc. which can be detected at a given temperature.
Dynamic range	Full range of solvent vapor conc. from detection limit to highest limiting conc. at a given temperature.
Resolution	Lowest conc. of the difference in solvent vapor conc. detected.
Response time	Time required to achieve a certain value from the baseline when step changes in solvent vapor conc. is applied.
Recovery time	Time taken by the sensor to return to the initial baseline when a step change in the vapor conc. is removed.
Hysteresis	The maximum difference in responses when the same vapor conc. is approached by increasing and decreasing the vapor conc. during the testing.
Life cycle	Total time over which the sensor is operating well.

To optimize the design of vapor sensors, ideal characteristics are low detection limit, small hysteresis, short response time, higher sensitivity and stability, selectivity towards specific vapours, and excellent stability. However, it is not easy to optimize all the properties at the same time. As a result, most research has been focused on improving selectivity and sensitivity which are not necessarily independent, while keeping other parameters at a constant level. Moreover, it is worth mentioning that all these ideal characteristics are not required at the same time in real-time applications. For example, the large dynamic range is not required in the context of leakage detection, similarly, short response time is not required in the realm of environment monitoring.

5.2. Brief Overview of Existing Capabilities of E-Noses

Since the precursor works of Persaud et al. [274] and Gardner et al. [275] more than thirty years ago, many researchers have tested the ability of e-noses to analyse patients' health through the volatolome. The use of e-noses was initially focused on the analysis of breath and the investigation of diseases pertaining to the lungs and stomach. But Wilson has made a good overview summarising the different diseases that can be diagnosed with a variety of commercial or prototypes e-noses, which are many [276–278]. A couple of commercial e-nose devices are emerging from the literature such as the JPL® from NASA [279], Fox 4000® from Alpha MOS [280], Nanose® from Nanose medical [61,281,282], or PEN® from Air Sense Analytics [283], but the most popular for health diagnosis from breaths analysis is the Cyranose® from Sensigent [284–286]. It is typically composed of an array of thirty-two conducting polymer nanocomposite (CPC) vapour sensors as shown in Figure 18. The sensors' data are processed by an inbuilt software and the analysis of the data is performed by PCA mapping. Sensigent claims the reproducibility and robustness of his Cyranose resulting from the quality of the training done with known VOCs.

Chapman et al. used the Cyranose 320 to detect malignant mesothelioma (MM) and asbestos-related diseases (ARDs) in patients [287]. The researchers have studied a total of thirty-eight patients with these diseases along with forty-two control subjects with the objective of obtaining their odour print. The e-nose demonstrated an efficiency of 95% and 88% to distinguish healthy controls from diseased patients of MM and ARD, respectively. Dragonieri et al. also used Cyranose 320 to discriminate asthma patients from healthy persons [288]. The researchers have tested the breath of forty people including patients and

controls. The results indicate that there is an evident difference between the breath prints of asthma patients and healthy controls.
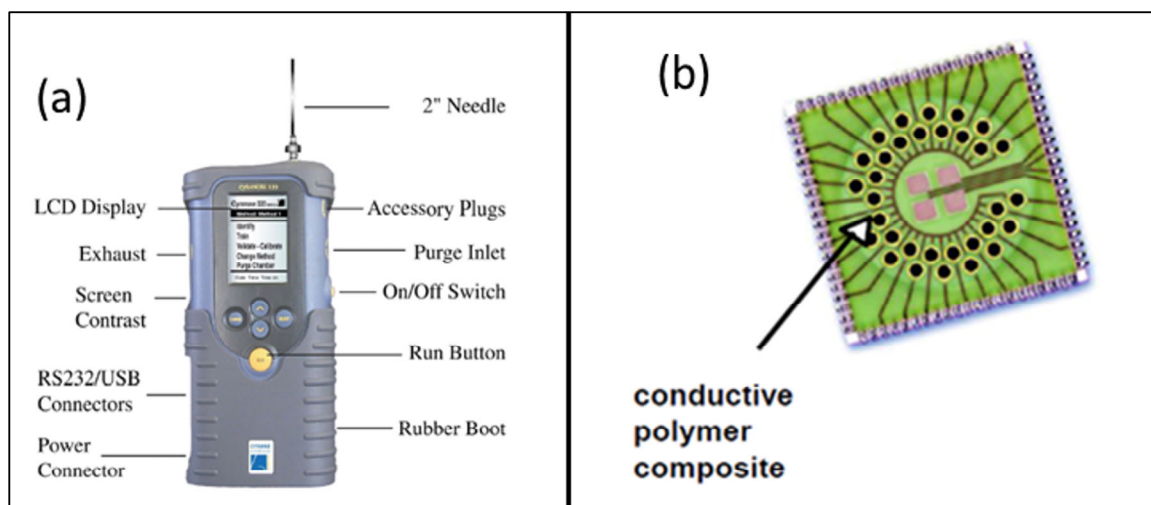

Figure 18. (**a**) Description of Cyranose, a commercial e-nose, and (**b**) CPC-based sensor array of the Cyranose [289].

Montuschi et al. used another kind of artificial nose based on an array of eight sensors made up of quartz crystal microbalance [290]. They tested twenty-seven atopic asthma patients and twenty-four healthy subjects. They compared the e-nose results with lung function test and fractional exhaled nitric oxide (FeNO) test. The findings of the study confirmed that the e-nose exhibited the highest level of discrimination ability compared to all other methods evaluated. The researchers have used both PCA and feed-forward neural networks for data interpretation. Different types of e-noses have been used for disease diagnosis as shown in Table 3. A more detailed review of sensing devices used for differential diagnosis, staging, and phenotyping of different categories of diseases has been made by Skotadis et al. [291].

Table 3. Different studies using e-noses to obtain the breath print of the human exhaled breath for various lung diseases (extracted from [65]).

Disease	Type of E-Nose	Nb of Sensors	Place of Tests	References
Asthma	Conducting polymer, quartz crystal microbalance	8–32	Australia, Italy, and The Netherlands	[287,288,290]
Lung cancer	Conducting polymer, quartz crystal microbalance, and calorimetric	8–36	USA and Italy	[211,268,292–294]
Tuberculosis	Surface acoustic wave and conducting polymer nanocomposite	1–14	Philippines, UK, and India	[295–297]

Furthermore, Lorwongtragool et al. developed a flexible wearable e-nose to monitor the VOCs released from human skin [298]. The e-nose was printed over the flexible poly(ethylene naphthalate) substrate, as shown in Figure 19a. The researchers have developed the sensors with CNT coated with different polymers including poly(vinyl chloride), poly(vinyl pyrrolidone), cumene-terminated poly(styrene-co-maleic anhydride), etc. They have attached a wireless Zig Bee system for data recording and transfer in the e-nose system. This wearable sensor array was able to classify the different types of body odours depending on the body activities and states such as running, walking, playing, and skin hygiene.

PCA was used in this classification as shown in Figure 19b. More recently, Haick et al. [299] have demonstrated the ability of a flexible e-nose to analyse the volatiles released by an absorber stuck on the skin of a rat to detect a biomarker (2-hydroxy-2-methyl-propanoic acid) and transduce its stress when submitted to an underwater trauma. A support vector machine (SVM) model allowed stress detection with an accuracy of 66 to 72% after machine learning had validated the computational stress model. Jiang et al. [300] report that piezo-electric nanogenerator (PENG) nanoarrays made of ZnO nanowires, CdS nanorods, and CuO/ZnO could autonomously detect H_2S at room temperature.
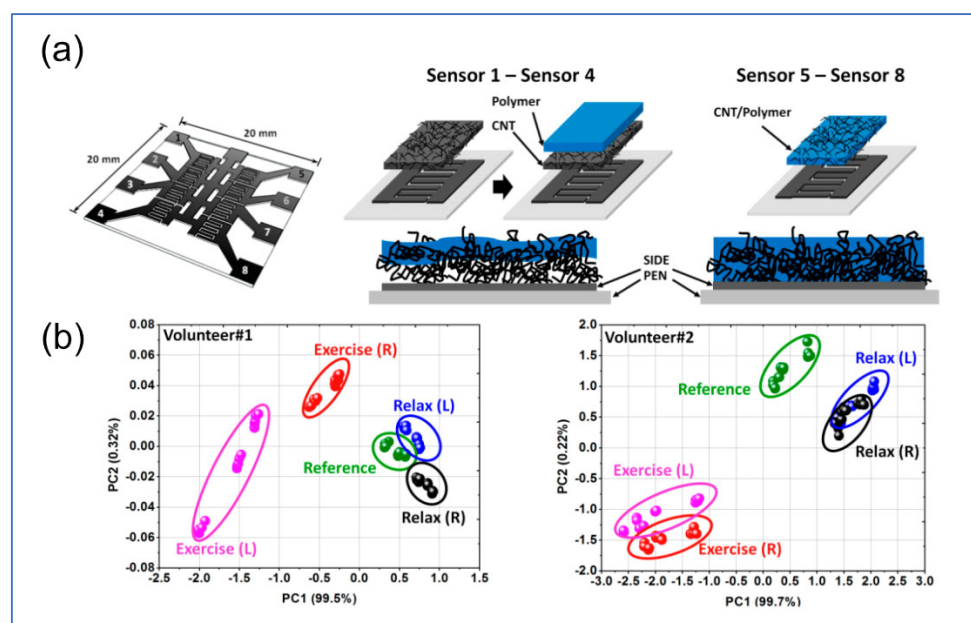
Figure 19. (**a**) Preparation of sensors' array for the wearable e-nose. (**b**) Discrimination of skin odour during various activities by the wearable e-nose using PCA [298].

5.3. Tailoring the Sensors' Selectivity to Improve the E-Nose Discrimination Ability

Feller et al. [171,301] employed a range of methodologies and strategies to improve both selectivity and sensitivity of polymer nanocomposite transducers for e-nose applications.

Kumar et al. tailored the junction gap between CNT to enhance the sensitivity and selectivity to organic vapours using the spray layer by layer (sLbL) method which allows precise adjustment of transducers' initial resistance and thickness. The junction gap between nanofillers (typically less than 15 nm) in percolated networks is a crucial parameter acting on tunnelling conduction that varies the resistance exponentially (Figure 20). The gap between carbon nanotubes in hydrophilic sensors can be tuned by cross-linking on their surface deacetylated chitosan macromolecules with non-covalent bonding [302] or by coiling around them amylose helices [303]. Apart from enhancing the transducer's sensitivity, Ar (also termed relative variation of resistance) by four to eight, a much stronger affinity for water, was obtained compared to the neat CNT. Further, the authors proposed two empiric models to predict the evolution of Ar with the strength of molecular interactions between the polymer used for the functionalization and the target analyte through the χ_{12} Flory–Huggins (XFH) interaction parameter [302] and to express the proportionality of Ar with the analyte content integrating the Langmuir–Henry Clustering (LHC) diffusion modes concept [304].

Figure 20. Schematic drawing of the sensing mechanism due to junction gap variation. (**a**) Initial gap in dry nitrogen. (**b**) Increased gap state in the presence of vapor molecules [305].

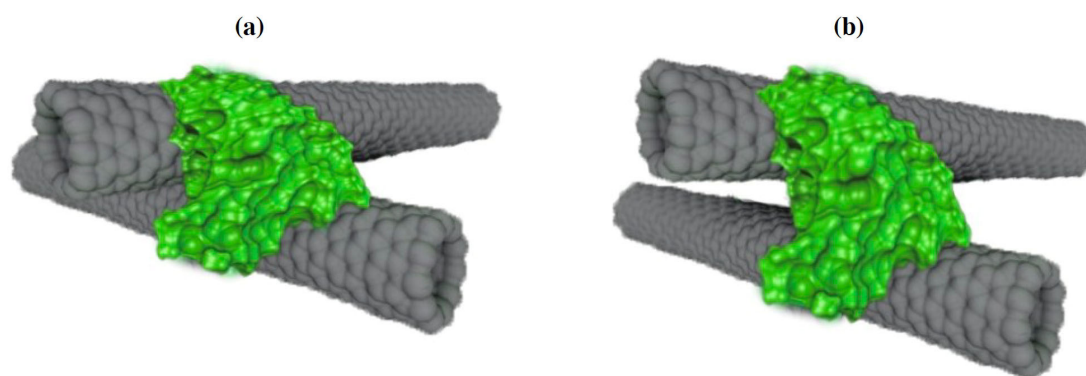At a larger scale than the distance between nanofillers, it is important to control the structure of the conducting architecture itself. Lu et al. [306] used the exclusion volumes of poly(methyl methacrylate) PMMA hard microbeads decorated with CNT to boost their sensitivity to methanol. A high sensitivity was achieved by focusing the disconnection of the CNT conducting network at contact points between the hard spheres. Other investigations were led to structure an interfacial CNT network with soft latex microbeads of a series of copolymers of acrylates of different welding ability. The resulting transducers were found to have a good selectivity to water [307].

Furthermore, Castro et al. fabricated by sLbL, a random network (RN) of carbon nanotubes (CNTs) further functionalized by drops of a PMMA, poly(lactic acid) PLA, poly(oxyethylene) POE, poly(carbonate) PC, and poly(caprolactone) PCL solutions, deposited directly on the RN to coat junctions. Principal component analysis (PCA) evidenced a very good discrimination of nine volatiles using an array of these five RN-functionalised sensors plus one with pure CNT [305]. These sensors exhibited a very high, fast, and reversible response Ar to acetone vapour. In addition, Lu et al. also developed Pani-CNT sensors with switchable polarity [308] and PC-CNT sensors to analyse the effects of vapour flow rate during detection, number of sprayed layers, and CNT content on the sensing behaviour of transducers [309].

S. Chatterjee et al. worked on the effect of surfactants (used to ensure an optimal dispersion of CNT in solution) on the sensing of organic volatiles identified as lung cancer biomarkers. Triton x405, sodium deoxycholate (DOC), sodium dodecylbenzene sulfonate (SDBS), and benzalkonium chloride (BnzlkCl) were the surfactants assembled in micelles on CNTs to cover their junctions; this functionalisation changed both the sensitivity and selectivity according to their chemical nature. The Triton x405-functionalised CNT transducer was sensitive to benzene and pentane, whereas the SDBS-functionalised CNT was more sensitive to ethanol, acetone, chloroform, and water, and the BnzlkCl-functionalised CNT responded better to n-pentane, isoprene, ethanol, and acetone vapours. A very good discrimination ability was clearly evidenced after PCA treatment. Alternatively, an e-nose made of PC-, PLA-, PS-, PCL-, and PMMA-functionalised CNT made by sLbL discriminated with 98% of the total variance by PCA, eighteen different polar and non-polar lung cancer biomarker vapours. This e-nose exhibited a minimum loss of data and discriminated easily acetone, isopropanol, butanone, cyclohexane, toluene, and benzene vapours [310,311].

Tung et al. investigated the input of graphene nanoplatelets to maximize the exchange surface with analytes in nanohybrid transducers for vapour sensing. The researchers have experienced a formulation of multiple conductive nanofillers including CNT, reduced graphene oxide (rGO) eventually stabilized with poly(1-vinyl-3-ethylimidazolium), a poly(ionic liquid) PIL, poly(3,4-ethylene dioxythiophene) PEDOT, an intrinsically conduct-

ing polymer, magnetic ferrite Fe_3O_4 and silver nanoparticles (AgNP). In a first combination of conducting fillers, a very good synergy of chemo-resistive properties was found between Fe_3O_4-decorated rGO hybridized with PEDOT and stabilized with PIL [198]. This transducer alone was able to classify well polar vapours (water, acetone, methanol, and ethanol) and to a lesser extent, non-polar vapours (toluene, dichlorobenzene, styrene, and chloroform). It had remarkably larger sensitivity than Fe_3O_4-decorated rGO hybridized with PEDOT or PEDOT-PIL alone. Moreover, another formulation based on AgNP-decorated rGO stabilized by PIL confirmed that graphene could reduce significantly the noise of signals and enhance the transducer's stability [196]. Additionally, it can be noticed that the substitution of Fe_3O_4 NP by AgNP to decorate graphene nanofoils had a similar effect on sensitivity increase but it did not change the selectivity of pure graphene towards methanol, ethanol, and methyl acetate. From this finding emerged the concept of "spacer"; graphene foils have very large surfaces and high conductivity but to make them sensitive to disconnection, it is necessary to intercalate them with particles to promote a "house of cards" conducting architecture.

S. Nag et al. focused on the detection of lung cancer biomarkers part of the volatolome using different spacers such as cyclodextrin or poly(sylsesquioxane). They worked mainly on the functionalization of polymers and nanomaterials to enhance the selectivity and sensitivity of transducers. In their study, the researchers have developed sensors based on cyclodextrin (CD) functionalized by amine, perbenzoyl and mannose sugar, and rGO [312]. CD was plugged with adamantane-functionalized pyrene bonded with exfoliated layers of rGO by π-π attractions to control the gap. These results suggested that sugar-functionalized CD was selective for methanol, amine-functionalized CD for acetone, and per benzylated CD for toluene, xylene, and benzene. The selectivity of sensors was well predicted by the XFH model. In addition, the researchers also developed chemically functionalized CNT with isooctyl-POSS and non-covalently modified CNT with phenyl-POSS [191]. POSS poly(hedral oligomeric silsesquioxane) is a spacer which can tailor the gap and conducting architecture. Chemical functionalization was carried out by acryloyl chloride functionalization of CNT followed by amidization with the anime group of POSS. Non-covalent attachments were obtained by π-π interactions between CNT and phenyl-POSS. Chemically grafted CNTs promoted good selectivity towards cyclohexane and pentane whereas non-covalently bonded CNTs showed selectivity for acetone, butanone, propanol, toluene, and ethanol. All chemo-resistive responses were well fitted using the XFH model. Moreover, highly sensitive methanol sensors were prepared using sulfonated poly(ether ether ketone) sPEEK with C_{60} fullerene and CNT nanohybrids. These sensors were able to detect 0.34 ppm of methanol with a very high signal-to-noise ratio (200) [313]. C_{60} used as a spacer in the CNT network was found to increase the sensitivity more than 2,5 times for almost all of the studied VOCs. This boosting effect of the C_{60} spacer was confirmed with both CNT and graphene hybrid conducting architectures, together with the remarkable stability brought by graphene at concentrations as low as 400 ppb [239].

Tripathi et al. demonstrated that it was possible to develop CPC volatile transducers with low environmental impact carbon nanofillers, such as nano-onions from diesel engine soot [314] or nano-rods synthesized from castor oil [175].

These examples highlight the diversity of combinations authorized by conductive polymer nanocomposites to transduce chemical information into a simple resistance variation signal and the promises they bring to enrich the detection spectrum of e-noses.

6. Conclusions & Prospects

This non-exhaustive review has focused on the different types of vapour sensors used for disease diagnosis such as lung or skin cancers from the analysis of volatiles

emitted by the body. Making an anticipated diagnosis simply by the analysis of exhaled breath, skin, or urine sounds very promising as it is non-invasive, low-cost, fast, and compatible with telemedicine. Considering the specific advantages and drawbacks of all available vapour sensors used to analyse the volatolome, it makes one think that conducting polymer nanocomposite-based transducers are among the most versatile and promising to satisfy the optimization requirements. Graphene, carbon nanotubes, carbon nanoparticles, fullerene, and their hybrids are very attractive for building easily disconnectable conductive hierarchical architectures. The variety of polymers and functional molecules used to tailor the morphology and chemical interactions at conducting junctions guarantees a wide range of detection of analytes. Spacer molecules like POSS or cyclodextrin and nano spacers like fullerenes proved to notably boost sensitivity. Chemical functional groups of polymers with different level of VAN DER WAALS and polar interactions used to tailor conducting junctions can interact and discriminate a wide range of volatiles emitted by the body and be considered as biomarkers of diseases. Combining these strategies proved to be effective at boosting the sensitivity and selectivity of sensor arrays (e-noses). Additionally, associating specific and non-specific transducers in the same arrays as in human olfaction can bring e-noses closer to the performances of their biological homologues. Moreover, taking benefit from the sensitivity to oxidizing gases of MOS and the fine selectivity of CPC to VAN DER WAALS interacting with VOC in the same sensors' array should allow them to deal with complex olfactive prints, such as those present in the volatolome analysed from the breath and skin.

The analysis of olfactive prints with statistical methods such as PCA or LDA to classify data and their subsequent processing in artificially neural networks demonstrated their power to give sense to the high level of complexity of signals delivered by e-noses. In this way, biomimicry can bring interesting solutions to the design of transducers and treatment algorithms (neuromorphic).

Although the reproducibility and sensitivity of sensors are being continuously improvised by the researchers, there are still challenges to reach enough robustness and reproducibility of signals to feed algorithms with reliable data. Controlling temperature or eventually correcting its effect on chemical signals can fix some issues, whereas it is more complex to deal with adsorption site poisonings in transducers, by H_2O [195] or H_2S [315] molecules, for instance. A compromise must be found between too strong and too week interactions between analytes and active molecules from the transducer, controlling the adsorption/desorption mechanism; selective filters can bring solutions but they also remove pertinent molecules to identify odours and prevent bias in the diagnosis. Hybrid materials can play an important role by synergising graphene stability, nanotubes interconnectivity, and spacers sensitivity when functionalized with polymers. Therefore, chemically modified hybrids with a well-defined architecture can solve the problem of reproducibility.

Data collection and sharing from e-noses and their interpretation are still challenging as there is no exchangeable protocol. For real-time applications, data analysis and result predictions must be improved by using trained neural network algorithms. But a huge amount of data for ill and healthy patients are required for the training of the ANN. Considering the constant progresses of computing power, e-noses with all these properties should be used in the close future for disease detection and diagnosis. Many clinical applications can result from the analysis of the volatolome with e-noses, potentially saving millions of lives on earth. This technique also has a tremendous potential to reduce the cost of treatments and diagnosis for fatal diseases which is very urgently needed in developing countries. Improvements of sensors to be more eco-friendly and bio-compatible (in skin VOC monitoring) can also be expected.

In future applications, nanosensor arrays analysing the volatolome will be integrated into wearable self-powered healthcare devices for clinical decision of prehospitalization [316]. This will also promote the development of telemedicine using monitoring platforms enabling wireless communication [317,318].

References

1. Ferlay, J.; Ervik, M.; Lam, F.; Laversanne, M.; Colombet, M.; Mery, L.; Piñeros, M.; Znaor, A.; Soerjomataram, I.; Bray, F. Cancer Today: Global Cancer Statistics in 2020. Available online: https://gco.iarc.who.int/today (accessed on 4 July 2024).
2. Dominioni, L.; Imperatori, A.; Rovera, F.; Ochetti, A.; Torrigiotti, G.; Paolucci, M. Stage I Nonsmall Cell Lung Carcinoma: Analysis of Survival and Implications for Screening. *Cancer* **2000**, *89*, 2334–2344. [CrossRef] [PubMed]
3. Alberg, A.J.; Ford, J.G.; Samet, J.M. Epidemiology of Lung Cancer: ACCP Evidence-Based Clinical Practice Guidelines (2nd Edition). *Chest* **2007**, *132*, 29S–55S. [CrossRef] [PubMed]
4. Jemal, A.; Siegel, R.; Ward, E.; Hao, Y.; Xu, J.; Thun, M.J. Cancer Statistics 2009. *CA Cancer J. Clin.* **2009**, *59*, 225–249. [CrossRef] [PubMed]
5. Siegel, R.L.; Miller, K.D.; Jemal, A. Cancer Statistics, 2015. *CA Cancer J. Clin.* **2015**, *65*, 5–29. [CrossRef]
6. Berg, C.D.; Aberle, D.R. CT Screening for Lung Cancer. *N. Engl. J. Med.* **2007**, *356*, 743–744; author reply 746–747.
7. New, M.; Keith, R. Early Detection and Chemoprevention of Lung Cancer. *F1000Research* **2018**, *7*, 61. [CrossRef]
8. Marks, R. An Overview of Skin Cancers. *Cancer* **1995**, *75*, 607–612. [CrossRef]
9. Schinke, C.; Mo, Y.; Yu, Y.; Amiri, K.; Sosman, J.; Greally, J.; Verma, A. Aberrant DNA Methylation in Malignant Melanoma. *Melanoma Res.* **2010**, *20*, 253–265. [CrossRef]
10. Balch, C.M.; Gershenwald, J.E.; Soong, S.J.; Thompson, J.F.; Atkins, M.B.; Byrd, D.R.; Buzaid, A.C.; Cochran, A.J.; Coit, D.G.; Ding, S.; et al. Final Version of 2009 AJCC Melanoma Staging and Classification. *J. Clin. Oncol.* **2009**, *27*, 6199–6206. [CrossRef]
11. Böni, R.; Schuster, C.; Nehrhoff, B.; Burg, G. Epidemiology of Skin Cancer. *Neuroendocrinol. Lett.* **2002**, *23*, 48–51. [CrossRef]
12. Han, J.; Qureshi, A.A.; Nan, H.; Zhang, J.; Song, Y.; Guo, Q.; Hunter, D.J. A Germline Variant in the Interferon Regulatory Factor 4 Gene as a Novel Skin Cancer Risk Locus. *Cancer Res.* **2011**, *71*, 1533–1539. [CrossRef] [PubMed]
13. Dancey, A.L.; Mahon, B.S.; Rayatt, S.S. A Review of Diagnostic Imaging in Melanoma. *J. Plast. Reconstr. Aesthet. Surg.* **2008**, *61*, 1275–1283. [CrossRef] [PubMed]
14. Tabár, L.; Yen, A.M.-F.; Wu, W.Y.-Y.; Chen, S.L.-S.; Chiu, S.Y.-H.; Fann, J.C.-Y.; Ku, M.M.-S.; Smith, R.A.; Duffy, S.W.; Chen, T.H.-H. Insights from the Breast Cancer Screening Trials: How Screening Affects the Natural History of Breast Cancer and Implications for Evaluating Service Screening Programs. *Breast J.* **2015**, *21*, 13–20. [CrossRef] [PubMed]
15. Tosteson, A.N.A.; Fryback, D.G.; Hammond, C.S.; Hanna, L.G.; Grove, M.R.; Brown, M.; Wang, Q.; Lindfors, K.; Pisano, E.D. Consequences of False-Positive Screening Mammograms. *JAMA Intern. Med.* **2014**, *174*, 954–961. [CrossRef]
16. American Cancer Society. *Cancer Facts & Figures 2015*; American Cancer Society: Atlanta, GA, USA, 2015; pp. 1–9.
17. Sone, S.; Nakayama, T.; Honda, T.; Tsushima, K.; Li, F.; Haniuda, M.; Takahashi, Y.; Suzuki, T.; Yamanda, T.; Kondo, R.; et al. Long-Term Follow-up Study of a Population-Based 1996-1998 Mass Screening Programme for Lung Cancer Using Mobile Low-Dose Spiral Computed Tomography. *Lung Cancer* **2007**, *58*, 329–341. [CrossRef]
18. Altintas, Z.; Tothill, I. Biomarkers and Biosensors for the Early Diagnosis of Lung Cancer. *Sens. Actuators B Chem.* **2013**, *188*, 988–998. [CrossRef]

19. Poli, D.; Carbognani, P.; Corradi, M.; Goldoni, M.; Acampa, O.; Balbi, B.; Bianchi, L.; Rusca, M.; Mutti, A. Exhaled Volatile Organic Compounds in Patients with Non-Small Cell Lung Cancer: Cross Sectional and Nested Short-Term Follow-up Study. *Respir. Res.* **2005**, *6*, 71. [CrossRef]

20. Sung, H.-J.; Cho, J.-Y. Biomarkers for the Lung Cancer Diagnosis and Their Advances in Proteomics. *BMB Rep.* **2008**, *41*, 615–625. [CrossRef]

21. Choi, Y.-E.; Kwak, J.-W.; Park, J.W. Nanotechnology for Early Cancer Detection. *Sensors* **2010**, *10*, 428–455. [CrossRef]

22. Bohunicky, B.; Mousa, S.A. Biosensors: The New Wave in Cancer Diagnosis. *Nanotechnol. Sci. Appl.* **2010**, *4*, 1–10. [CrossRef]

23. Lollo, G.; Rivera-Rodriguez, G.R.; Bejaud, J.; Montier, T.; Passirani, C.; Benoit, J.-P.; García-Fuentes, M.; Alonso, M.J.; Torres, D. Polyglutamic Acid–PEG Nanocapsules as Long Circulating Carriers for the Delivery of Docetaxel. *Eur. J. Pharm. Biopharm.* **2014**, *87*, 47–54. [CrossRef] [PubMed]

24. Bach, P.B.; Mirkin, J.N.; Oliver, T.K.; Azzoli, C.G.; Berry, D.; Brawley, O.W.; Byers, T.; Colditz, G.A.; Gould, M.K.; Jett, J.R.; et al. Benefits and Harms of CT Screening for Lung Cancer: A Systematic Review. *JAMA* **2012**, *307*, 2418–2429. [CrossRef] [PubMed]

25. Wender, R.; Fontham, E.T.H.; Barrera, E.; Colditz, G.A.; Church, T.R.; Ettinger, D.S.; Etzioni, R.; Flowers, C.R.; Gazelle, G.S.; Kelsey, D.K.; et al. American Cancer Society Lung Cancer Screening Guidelines. *CA Cancer J. Clin.* **2013**, *63*, 107–117. [CrossRef] [PubMed]

26. De Koning, H.J.; Meza, R.; Plevritis, S.K.; Haaf, K.T.; Munshi, V.N.; Jeon, J.; Erdogan, S.A.; Kong, C.Y.; Han, S.S.; Van Rosmalen, J.; et al. Benefits and Harms of CT Lung Cancer Screening Strategies. A Comparative Modeling Study for the U.S. Preventive Services Task Force. *Ann. Intern. Med.* **2014**, *160*, 311–320. [CrossRef]

27. Moyer, V.A.; US Preventive Services Task Force. Screening for Lung Cancer: U.S. Preventive Services Task Force Recommendation Statement. *Ann. Intern. Med.* **2014**, *160*, 330–338. [CrossRef]

28. Detterbeck, F.C.; Mazzone, P.J.; Naidich, D.P.; Bach, P.B. Screening for Lung Cancer: Diagnosis and Management of Lung Cancer, 3rd ed: American College of Chest Physicians Evidence-Based Clinical Practice Guidelines. *Chest* **2013**, *143*, e78S–e92S. [CrossRef]

29. Jaklitsch, M.T.; Jacobson, F.L.; Austin, J.H.M.; Field, J.K.; Jett, J.R.; Keshavjee, S.; MacMahon, H.; Mulshine, J.L.; Munden, R.F.; Salgia, R.; et al. The American Association for Thoracic Surgery Guidelines for Lung Cancer Screening Using Low-Dose Computed Tomography Scans for Lung Cancer Survivors and Other High-Risk Groups. *J. Thorac. Cardiovasc. Surg.* **2012**, *144*, 33–38. [CrossRef]

30. Wood, D.E.; Kazerooni, E.; Baum, S.L.; Dransfield, M.T.; Eapen, G.A.; Ettinger, D.S.; Hou, L.; Jackman, D.M.; Klippenstein, D.; Kumar, R.; et al. Lung Cancer Screening, Version 1.2015. *J. Natl. Compr. Cancer Netw.* **2015**, *13*, 23–34. [CrossRef]

31. Patz, E.F.; Swensen, S.J.; Herndon, J.E. Estimate of Lung Cancer Mortality from Low-Dose Spiral Computed Tomography Screening Trials: Implications for Current Mass Screening Recommendations. *J. Clin. Oncol.* **2004**, *22*, 2202–2206. [CrossRef]

32. Goto, I.; Yoneda, S.; Yamamoto, M.; Kawajiri, K. Prognostic Significance of Germ Line Polymorphisms of the CYP1A1 and Glutathione S-Transferase Genes in Patients with Non-Small Cell Lung Cancer. *Cancer Res.* **1996**, *56*, 3725–3730.

33. Chen, X.; Muhammad, K.G.; Madeeha, C.; Fu, W.; Xu, L.; Hu, Y.; Liu, J.; Ying, K.; Chen, L.; Yurievna, G.O. Calculated Indices of Volatile Organic Compounds (VOCs) in Exhalation for Lung Cancer Screening and Early Detection. *Lung Cancer* **2021**, *154*, 197–205. [CrossRef] [PubMed]

34. Smolinska, A.; Hauschild, A.C.; Fijten, R.R.R.; Dallinga, J.W.; Baumbach, J.; van Schooten, F.J. Current Breathomics—A Review on Data Pre-Processing Techniques and Machine Learning in Metabolomics Breath Analysis. *J. Breath Res.* **2014**, *8*, 027105. [CrossRef] [PubMed]

35. Tisch, U.; Haick, H. Chemical Sensors for Breath Gas Analysis: The Latest Developments at the Breath Analysis Summit 2013. *J. Breath Res.* **2014**, *8*, 27103. [CrossRef]

36. Freddi, S.; Emelianov, A.V.; Bobrinetskiy, I.I.; Drera, G.; Pagliara, S.; Kopylova, D.S.; Chiesa, M.; Santini, G.; Mores, N.; Moscato, U.; et al. Development of a Sensing Array for Human Breath Analysis Based on SWCNT Layers Functionalized with Semiconductor Organic Molecules. *Adv. Health Mater.* **2020**, *9*, e2000377. [CrossRef]

37. Freddi, S.; Sangaletti, L. Trends in the Development of Electronic Noses Based on Carbon Nanotubes Chemiresistors for Breathomics. *Nanomaterials* **2022**, *12*, 2992. [CrossRef]

38. Scheideler, L.; Manke, H.G.; Schwulera, U.; Inacker, O.; Hämmerle, H. Detection of Nonvolatile Macromolecules in Breath. A Possible Diagnostic Tool? *Am. Rev. Respir. Dis.* **1993**, *148*, 778–784. [CrossRef]

39. Pauling, L.; Robinson, B.; Teranishi, R.; Cary, P. Quantitative Analysis of Urine Vapor and Breath by Gas-Liquid Partition Chromatography. *Proc. Natl. Acad. Sci. USA* **1971**, *68*, 2374–2376. [CrossRef]

40. Broza, Y.Y.; Zuri, L.; Haick, H. Combined Volatolomics for Monitoring of Human Body Chemistry. *Sci. Rep.* **2014**, *4*, 4611. [CrossRef]

41. de Lacy Costello, B.; Amann, A.; Al-Kateb, H.; Flynn, C.; Filipiak, W.; Khalid, T.; Osborne, D.; Ratcliffe, N.M. A Review of the Volatiles from the Healthy Human Body. *J. Breath Res.* **2014**, *8*, 014001. [CrossRef]

42. Miekisch, W.; Schubert, J.K.; Noeldge-Schomburg, G.F.E. Diagnostic Potential of Breath Analysis—Focus on Volatile Organic Compounds. *Clin. Chim. Acta* **2004**, *347*, 25–39. [CrossRef]

43. Cheng, W.-H.; Lee, W.-J. Technology Development in Breath Microanalysis for Clinical Diagnosis. *J. Lab. Clin. Med.* **1999**, *133*, 218–228. [CrossRef] [PubMed]

44. Yu, J.B.; Byun, H.G.; So, M.S.; Huh, J.S. Analysis of Diabetic Patient's Breath with Conducting Polymer Sensor Array. *Sens. Actuators B Chem.* **2005**, *108*, 305–308. [CrossRef]

45. Trotter, M.D.; Sulway, M.J.; Trotter, E. The Rapid Determination of Acetone in Breath and Plasma. *Clin. Chim. Acta* **1971**, *35*, 137–143. [CrossRef] [PubMed]

46. Dawson, J.; Green, K.; Lazarowicz, H.; Cornford, P.; Probert, C. Analysis of Urinary Volatile Organic Compounds for Prostate Cancer Diagnosis: A Systematic Review. *BJUI Compass* **2024**, *5*, 936–947. [CrossRef]

47. Cornu, J.N.; Cancel-Tassin, G.; Ondet, V.; Girardet, C.; Cussenot, O. Olfactory Detection of Prostate Cancer by Dogs Sniffing Urine: A Step Forward in Early Diagnosis. *Eur. Urol.* **2011**, *59*, 197–201. [CrossRef]

48. Španěl, P.; Smith, D.; Holland, T.A.; Singary, W.A.; Elder, J.B. Analysis of Formaldehyde in the Headspace of Urine from Bladder and Prostate Cancer Patients Using Selected Ion Flow Tube Mass Spectrometry. *Rapid Commun. Mass. Spectrom.* **1999**, *13*, 1354–1359. [CrossRef]

49. Cikach, F.S.; Dweik, R.A. Cardiovascular Biomarkers in Exhaled Breath. *Prog. Cardiovasc. Dis.* **2012**, *55*, 34–43. [CrossRef]

50. Dummer, J.; Storer, M.; Swanney, M.; McEwan, M.; Scott-Thomas, A.; Bhandari, S.; Chambers, S.; Dweik, R.; Epton, M. Analysis of Biogenic Volatile Organic Compounds in Human Health and Disease. *TrAC Trends Anal. Chem.* **2011**, *30*, 960–967. [CrossRef]

51. Kischkel, S.; Miekisch, W.; Sawacki, A.; Straker, E.M.; Trefz, P.; Amann, A.; Schubert, J.K. Breath biomarkers for lung cancer detection and assessment of smoking related effects-confounding variables, influence of normalization and statistical algorithms. *Clin. Chim. Acta* **2010**, *411*, 1637–1644. [CrossRef]

52. Pleil, J.D.; Lindstrom, A.B. Exhaled Human Breath Measurement Method for Assessing Exposure to Halogenated Volatile Organic Compounds. *Clin. Chem.* **1997**, *43*, 723–730. [CrossRef]

53. Wallace, L.A.; Pellizzari, E.D. Recent Advances in Measuring Exhaled Breath and Estimating Exposure and Body Burden for Volatile Organic Compounds (VOCs). *Environ. Health Perspect.* **1995**, *103*, 95–98. [CrossRef] [PubMed]

54. Wallace, L.; Buckley, T.; Pellizzari, E.; Gordon, S. Breath Measurements as Volatile Organic Compound Biomarkers. *Environ. Health Perspect.* **1996**, *104*, 861–869. [CrossRef] [PubMed]

55. Aghdassi, E.; Allard, J.P. Breath Alkanes as a Marker of Oxidative Stress in Different Clinical Conditions. *Free Radic. Biol. Med.* **2000**, *28*, 880–886. [CrossRef] [PubMed]

56. Stone, B.G.; Besse, T.J.; Duane, W.C.; Evans, C.D.; DeMaster, E.G. Effect of Regulating Cholesterol Biosynthesis on Breath Isoprene Excretion in Men. *Lipids* **1993**, *28*, 705–708. [CrossRef]

57. Lebovitz, H.E. Diabetic Ketoacidosis. *Lancet* **1995**, *345*, 767–772. [CrossRef]

58. Cope, K.; Risby, T.; Diehl, A.M. Increased Gastrointestinal Ethanol Production in Obese Mice: Implications for Fatty Liver Disease Pathogenesis. *Gastroenterology* **2000**, *119*, 1340–1347. [CrossRef]

59. Davis, P.L.; Dal Cortivo, L.A.; Maturo, J. Endogenous Isopropanol: Forensic and Biochemical Implications. *J. Anal. Toxicol.* **1984**, *8*, 209–212. [CrossRef]

60. Davies, S.; Spanel, P.; Smith, D. Quantitative Analysis of Ammonia on the Breath of Patients in End-Stage Renal Failure. *Kidney Int.* **1997**, *52*, 223–228. [CrossRef]

61. Nakhleh, M.K.; Haick, H.; Humbert, M.; Cohen-Kaminsky, S. Volatolomics of Breath as an Emerging Frontier in Pulmonary Arterial Hypertension. *Eur. Respir. J.* **2017**, *49*, 1601897. [CrossRef]

62. Wilson, A.D.; Baietto, M. Advances in Electronic-Nose Technologies Developed for Biomedical Applications. *Sensors* **2011**, *11*, 1105–1176. [CrossRef]

63. Novak, B.J.; Blake, D.R.; Meinardi, S.; Rowland, F.S.; Pontello, A.; Cooper, D.M.; Galassetti, P.R. Exhaled Methyl Nitrate as a Noninvasive Marker of Hyperglycemia in Type 1 Diabetes. *Proc. Natl. Acad. Sci. USA* **2007**, *104*, 15613–15618. [CrossRef] [PubMed]

64. Wehinger, A.; Schmid, A.; Mechtcheriakov, S.; Ledochowski, M.; Grabmer, C.; Gastl, G.A.; Amann, A. Lung Cancer Detection by Proton Transfer Reaction Mass-Spectrometric Analysis of Human Breath Gas. *Int. J. Mass. Spectrom.* **2007**, *265*, 49–59. [CrossRef]

65. Wilson, A. Advances in Electronic-Nose Technologies for the Detection of Volatile Biomarker Metabolites in the Human Breath. *Metabolites* **2015**, *5*, 140–163. [CrossRef]

66. Broza, Y.Y.; Kremer, R.; Tisch, U.; Gevorkyan, A.; Shiban, A.; Best, L.A.; Haick, H. A Nanomaterial-Based Breath Test for Short-Term Follow-up after Lung Tumor Resection. *Nanomedicine* **2013**, *9*, 15–21. [CrossRef]

67. Preti, G.; Labows, J.N.; Kostelc, J.G.; Aldinger, S.; Daniele, R. Analysis of Lung Air from Patients with Bronchogenic Carcinoma and Controls Using Gas Chromatography-Mass Spectrometry. *J. Chromatogr. B Biomed. Sci. Appl.* **1988**, *432*, 1–11. [CrossRef]

68. Horváth, I.; Lázár, Z.; Gyulai, N.; Kollai, M.; Losonczy, G. Exhaled Biomarkers in Lung Cancer. *Eur. Respir. J.* **2009**, *34*, 261–275. [CrossRef]

69. Chen, X.; Xu, F.; Wang, Y.; Pan, Y.; Lu, D.; Wang, P.; Ying, K.; Chen, E.; Zhang, W. A Study of the Volatile Organic Compounds Exhaled by Lung Cancer Cells in Vitro for Breath Diagnosis. *Cancer* **2007**, *110*, 835–844. [CrossRef]

70. Zhang, Z.-M.; Cai, J.-J.; Ruan, G.-H.; Li, G.-K. The Study of Fingerprint Characteristics of the Emanations from Human Arm Skin Using the Original Sampling System by SPME-GC/MS. *J. Chromatogr. B* **2005**, *822*, 244–252. [CrossRef]

71. Bernier, U.R.; Kline, D.L.; Barnard, D.R.; Schreck, C.E.; Yost, R.A. Analysis of Human Skin Emanations by Gas Chromatography/Mass Spectrometry. 2. Identification of Volatile Compounds That Are Candidate Attractants for the Yellow Fever Mosquito (Aedes Aegypti). *Anal. Chem.* **2000**, *72*, 747–756. [CrossRef]

72. Acevedo, C.A.; Sanchez, E.Y.; Reyes, J.G.; Young, M.E. Volatile Profiles of Human Skin Cell Cultures in Different Degrees of Senescence. *J. Chromatogr. B* **2010**, *878*, 449–455. [CrossRef]

73. Shirasu, M.; Touhara, K. The Scent of Disease: Volatile Organic Compounds of the Human Body Related to Disease and Disorder. *J. Biochem.* **2011**, *150*, 257–266. [CrossRef] [PubMed]

74. Dent, A.G.; Sutedja, T.G.; Zimmerman, P. V Exhaled Breath Analysis for Lung Cancer. *J. Thorac. Dis.* **2013**, *5*, S540–S550. [CrossRef] [PubMed]

75. Rana, S.; Singla, A.K.; Bajaj, A.; Elci, S.G.; Miranda, O.R.; Mout, R.; Yan, B.; Jirik, F.R.; Rotello, V.M. Array-Based Sensing of Metastatic Cells and Tissues Using Nanoparticle–Fluorescent Protein Conjugates. *ACS Nano* **2012**, *6*, 8233–8240. [CrossRef] [PubMed]

76. Pavlou, A.K.; Magan, N.; Sharp, D.; Brown, J.; Barr, H.; Turner, A.P.F. An Intelligent Rapid Odour Recognition Model in Discrimination of Helicobacter Pylori and Other Gastroesophageal Isolates in Vitro. *Biosens. Bioelectron.* **2000**, *15*, 333–342. [CrossRef] [PubMed]

77. Manolis, A. The Diagnostic Potential of Breath Analysis. *Clin. Chem.* **1983**, *29*, 5–15. [CrossRef]

78. Williams, H.; Pembroke, A. Sniffer Dogs in the Melanoma Clinic? *Lancet* **1989**, *333*, 734. [CrossRef]

79. Church, J.; Williams, H. Another Sniffer Dog for the Clinic? *Lancet* **2001**, *358*, 930. [CrossRef]

80. D'Amico, A.; Bono, R.; Pennazza, G.; Santonico, M.; Mantini, G.; Bernabei, M.; Zarlenga, M.; Roscioni, C.; Martinelli, E.; Paolesse, R.; et al. Identification of Melanoma with a Gas Sensor Array. *Ski. Res. Technol.* **2008**, *14*, 226–236. [CrossRef]

81. Kwak, J.; Gallagher, M.; Ozdener, M.H.; Wysocki, C.J.; Goldsmith, B.R.; Isamah, A.; Faranda, A.; Fakharzadeh, S.S.; Herlyn, M.; Johnson, A.T.C.; et al. Volatile Biomarkers from Human Melanoma Cells. *J. Chromatogr. B* **2013**, *931*, 90–96. [CrossRef]

82. Abaffy, T.; Möller, M.G.; Riemer, D.D.; Milikowski, C.; DeFazio, R.A. Comparative Analysis of Volatile Metabolomics Signals from Melanoma and Benign Skin: A Pilot Study. *Metabolomics* **2013**, *9*, 998–1008. [CrossRef]

83. Paliwal, S.; Hwang, B.H.; Tsai, K.Y.; Mitragotri, S. Diagnostic Opportunities Based on Skin Biomarkers. *Eur. J. Pharm. Sci.* **2013**, *50*, 546–556. [CrossRef] [PubMed]

84. Hiroshi, K.; Masaya, H.; Nariyoshi, S.; Makoto, M. Evaluation of Volatile Sulfur Compounds in the Expired Alveolar Gas in Patients with Liver Cirrhosis. *Clin. Chim. Acta* **1978**, *85*, 279–284. [CrossRef] [PubMed]

85. Acevedo, C.A.; Sanchez, E.Y.; Reyes, J.G.; Young, M.E. Volatile Organic Compounds Produced by Human Skin Cells. *Biol. Res.* **2007**, *40*, 347–355. [CrossRef] [PubMed]

86. Nose, K.; Ueda, H.; Ohkuwa, T.; Kondo, T.; Araki, S.; Ohtani, H.; Tsuda, T. Identification and Assessment of Carbon Monoxide in Gas Emanated from Human Skin. *Chromatography* **2006**, *27*, 27–29.

87. Simenhoff, M.L.; Burke, J.F.; Saukkonen, J.J.; Ordinario, A.T.; Doty, R.; Dunn, S. Biochemical Profile of Uremic Breath. *N. Engl. J. Med.* **1977**, *297*, 132–135. [CrossRef]

88. Meinardi, S.; Jin, K.B.; Barletta, B.; Blake, D.R.; Vaziri, N.D. Exhaled Breath and Fecal Volatile Organic Biomarkers of Chronic Kidney Disease. *Biochim. Biophys. Acta (BBA)-Gen. Subj.* **2012**, *1830*, 2531–2537. [CrossRef]

89. Zilberman, Y.; Tisch, U.; Shuster, G.; Pisula, W.; Feng, X.; Müllen, K.; Haick, H. Carbon Nanotube/Hexa-Peri-Hexabenzocoronene Bilayers for Discrimination between Nonpolar Volatile Organic Compounds of Cancer and Humid Atmospheres. *Adv. Mater.* **2010**, *22*, 4317–4320. [CrossRef]

90. Mashir, A.; Dweik, R.A. Exhaled Breath Analysis: The New Interface between Medicine and Engineering. *Adv. Powder Technol.* **2009**, *20*, 420–425. [CrossRef]

91. Ionescu, R.; Broza, Y.Y.; Shaltieli, H.; Sadeh, D.; Zilberman, Y.; Feng, X.; Glass-Marmor, L.; Lejbkowicz, I.; Müllen, K.; Miller, A.; et al. Detection of Multiple Sclerosis from Exhaled Breath Using Bilayers of Polycyclic Aromatic Hydrocarbons and Single-Wall Carbon Nanotubes. *ACS Chem. Neurosci.* **2011**, *2*, 687–693. [CrossRef]

92. Xu, Z.Q.; Broza, Y.Y.; Ionscu, R.; Tisch, U.; Ding, L.; Liu, H.; Song, Q.; Pan, Y.Y.; Xiong, F.X.; Gu, K.S.; et al. A Nanomaterial-Based Breath Test for Distinguishing Gastric Cancer from Benign Gastric Conditions. *Br. J. Cancer* **2013**, *108*, 941–950. [CrossRef]

93. Santonico, M.; Lucantoni, G.; Pennazza, G.; Capuano, R.; Galluccio, G.; Roscioni, C.; La Delfa, G.; Consoli, D.; Martinelli, E.; Paolesse, R.; et al. In Situ Detection of Lung Cancer Volatile Fingerprints Using Bronchoscopic Air-Sampling. *Lung Cancer* **2012**, *77*, 46–50. [CrossRef] [PubMed]

94. Turner, C.; Knobloch, H.; Richards, J.; Richards, P.; Mottram, T.T.F.; Marlin, D.; Chambers, M.A. Development of a Device for Sampling Cattle Breath. *Biosyst. Eng.* **2012**, *112*, 75–81. [CrossRef]

95. Bruins, M.; Rahim, Z.; Bos, A.; van de Sande, W.W.J.; Endtz, H.P.; van Belkum, A. Diagnosis of Active Tuberculosis by E-Nose Analysis of Exhaled Air. *Tuberculosis* **2013**, *93*, 232–238. [CrossRef]

96. Wlodzimirow, K.A.; Abu-Hanna, A.; Schultz, M.J.; Maas, M.A.W.; Bos, L.D.J.; Sterk, P.J.; Knobel, H.H.; Soers, R.J.T.; Chamuleau, R.A.F.M. Exhaled Breath Analysis with Electronic Nose Technology for Detection of Acute Liver Failure in Rats. *Biosens. Bioelectron.* **2014**, *53*, 129–134. [CrossRef]

97. Tisch, U.; Schlesinger, I.; Ionescu, R.; Nassar, M.; Axelrod, N.; Robertman, D.; Tessler, Y.; Azar, F.; Marmur, A.; Aharon-Peretz, J.; et al. Detection of Alzheimer's and Parkinson's Disease from Exhaled Breath Using Nanomaterial-Based Sensors. *Nanomedicine* **2012**, *8*, 43–56. [CrossRef]

98. Ho, C.; Robinson, A.; Miller, D.; Davis, M. Overview of Sensors and Needs for Environmental Monitoring. *Sensors* **2005**, *5*, 4–37. [CrossRef]

99. Lamagna, A.; Reich, S.; Rodríguez, D.; Boselli, A.; Cicerone, D. The Use of an Electronic Nose to Characterize Emissions from a Highly Polluted River. *Sens. Actuators B Chem.* **2008**, *131*, 121–124. [CrossRef]

100. Su, S.; Wu, W.; Gao, J.; Lu, J.; Fan, C. Nanomaterials-Based Sensors for Applications in Environmental Monitoring. *J. Mater. Chem.* **2012**, *22*, 18101–18110. [CrossRef]

101. Camara, E.H.M.; Breuil, P.; Briand, D.; de Rooij, N.F.; Pijolat, C. A Micro Gas Preconcentrator with Improved Performance for Pollution Monitoring and Explosives Detection. *Anal. Chim. Acta* **2011**, *688*, 175–182. [CrossRef]

102. Liu, Q.; Zhou, Q.; Jiang, G. Nanomaterials for Analysis and Monitoring of Emerging Chemical Pollutants. *TrAC Trends Anal. Chem.* **2014**, *58*, 10–22. [CrossRef]

103. Gibson, T.D.; Prosser, O.; Hulbert, J.N.; Marshall, R.W.; Corcoran, P.; Lowery, P.; Ruck-Keene, E.A.; Heron, S. Detection and Simultaneous Identification of Microorganisms from Headspace Samples Using an Electronic Nose. *Sens. Actuators B Chem.* **1997**, *44*, 413–422. [CrossRef]

104. Fleming-Jones, M.E.; Smith, R.E. Volatile Organic Compounds in Foods: A Five Year Study. *J. Agric. Food Chem.* **2003**, *51*, 8120–8127. [CrossRef] [PubMed]

105. Ampuero, S.; Bosset, J.O. The Electronic Nose Applied to Dairy Products: A Review. *Sens. Actuators B Chem.* **2003**, *94*, 1–12. [CrossRef]

106. Ghasemi-Varnamkhasti, M.; Mohtasebi, S.S.; Siadat, M.; Balasubramanian, S. Meat Quality Assessment by Electronic Nose (Machine Olfaction Technology). *Sensors* **2009**, *9*, 6058–6083. [CrossRef]

107. Ragazzo-Sanchez, J.A.; Chalier, P.; Chevalier, D.; Ghommidh, C. Electronic Nose Discrimination of Aroma Compounds in Alcoholised Solutions. *Sens. Actuators B Chem.* **2006**, *114*, 665–673. [CrossRef]

108. Kumar, A.; Castro, M.; Feller, J.F. Review on sensor array-based analytical technologies for quality control of food and beverages. *Sensors* **2023**, *23*, 4017. [CrossRef]

109. Haddi, Z.; Mabrouk, S.; Bougrini, M.; Tahri, K.; Sghaier, K.; Barhoumi, H.; El Bari, N.; Maaref, A.; Jaffrezic-Renault, N.; Bouchikhi, B. E-Nose and e-Tongue Combination for Improved Recognition of Fruit Juice Samples. *Food Chem.* **2014**, *150*, 246–253. [CrossRef]

110. Sobański, T.; Szczurek, a.; Nitsch, K.; Licznerski, B.W.; Radwan, W. Electronic Nose Applied to Automotive Fuel Qualification. *Sens. Actuators B Chem.* **2006**, *116*, 207–212. [CrossRef]

111. Benvenho, A.R.V.; Li, R.W.C.; Gruber, J. Polymeric Electronic Gas Sensor for Determining Alcohol Content in Automotive Fuels. *Sens. Actuators B Chem.* **2009**, *136*, 173–176. [CrossRef]

112. Ermanok, R.; Assad, O.; Zigelboim, K.; Wang, B.; Haick, H. Discriminative Power of Chemically Sensitive Silicon Nanowire Field Effect Transistors to Volatile Organic Compounds. *ACS Appl. Mater. Interfaces* **2013**, *5*, 11172–11183. [CrossRef]

113. Li, B.; Sauvé, G.; Iovu, M.C.; Jeffries-El, M.; Zhang, R.; Cooper, J.; Santhanam, S.; Schultz, L.; Revelli, J.C.; Kusne, A.G.; et al. Volatile Organic Compound Detection Using Nanostructured Copolymers. *Nano Lett.* **2006**, *6*, 1598–1602. [CrossRef] [PubMed]

114. Toal, S.J.; Trogler, W.C. Polymer Sensors for Nitroaromatic Explosives Detection. *J. Mater. Chem.* **2006**, *16*, 2871–2883. [CrossRef]

115. Pleil, J.D.; Smith, L.B.; Zelnick, S.D. Personal Exposure to JP-8 Jet Fuel Vapors and Exhaust at Air Force Bases. *Environ. Health Perspect.* **2000**, *108*, 183–192. [CrossRef] [PubMed]

116. Mochalski, P.; Wzorek, B.; Śliwka, I.; Amann, A. Suitability of Different Polymer Bags for Storage of Volatile Sulphur Compounds Relevant to Breath Analysis. *J. Chromatogr. B* **2009**, *877*, 189–196. [CrossRef]

117. Gilchrist, F.J.; Razavi, C.; Webb, A.K.; Jones, A.M.; Španěl, P.; Smith, D.; Lenney, W. An Investigation of Suitable Bag Materials for the Collection and Storage of Breath Samples Containing Hydrogen Cyanide. *J. Breath Res.* **2012**, *6*, 036004. [CrossRef]

118. Beauchamp, J.; Herbig, J.; Gutmann, R.; Hansel, A. On the Use of Tedlar® Bags for Breath-Gas Sampling and Analysis. *J. Breath Res.* **2008**, *2*, 046001. [CrossRef]

119. Schubert, J.K.; Spittler, K.H.; Braun, G.; Geiger, K.; Guttmann, J. CO_2-Controlled Sampling of Alveolar Gas in Mechanically Ventilated Patients. *J. Appl. Physiol.* **2001**, *90*, 486–492. [CrossRef]

120. Miekisch, W.; Kischkel, S.; Sawacki, A.; Liebau, T.; Mieth, M.; Schubert, J.K. Impact of Sampling Procedures on the Results of Breath Analysis. *J. Breath Res.* **2008**, *2*, 026007. [CrossRef]

121. Bikov, A.; Paschalaki, K.; Logan-Sinclair, R.; Horváth, I.; Kharitonov, S.A.; Barnes, P.J.; Usmani, O.S.; Paredi, P. Standardised Exhaled Breath Collection for the Measurement of Exhaled Volatile Organic Compounds by Proton Transfer Reaction Mass Spectrometry. *BMC Pulm. Med.* **2013**, *13*, 43. [CrossRef]

122. Pleil, J.D.; Lindstrom, A.B. Measurement of Volatile Organic Compounds in Exhaled Breath as Collected in Evacuated Electropolished Canisters. *J. Chromatogr. B Biomed. Sci. Appl.* **1995**, *665*, 271–279. [CrossRef]

123. Mieth, M.; Schubert, J.K.; Gröger, T.; Sabei, B.; Kischkel, S.; Fuchs, P.; Hein, D.; Zimmermann, R.; Miekisch, W. Automated Needle Trap Heart-Cut GC/MS and Needle Trap Comprehensive Two-Dimensional GC/TOF-MS for Breath Gas Analysis in the Clinical Environment. *Anal. Chem.* **2010**, *82*, 2541–2551. [CrossRef]

124. Knutson, M.D.; Viteri, F.E. Concentrating Breath Samples Using Liquid Nitrogen: A Reliable Method for the Simultaneous Determination of Ethane and Pentane. *Anal. Biochem.* **1996**, *242*, 129–135. [CrossRef] [PubMed]

125. Grote, C.; Pawliszyn, J. Solid-Phase Microextraction for the Analysis of Human Breath. *Anal. Chem.* **1997**, *69*, 587–596. [CrossRef] [PubMed]

126. Risby, T.H.; Sehnert, S.S. Clinical Application of Breath Biomarkers of Oxidative Stress Status. *Free Radic. Biol. Med.* **1999**, *27*, 1182–1192. [CrossRef]

127. Raymer, J.H.; Thomas, K.W.; Cooper, S.D.; Whitaker, D.A.; Pellizzari, E.D. A Device for Sampling of Human Alveolar Breath for the Measurement of Expired Volatile Organic Compounds. *J. Anal. Toxicol.* **1990**, *14*, 337–344. [CrossRef]

128. Turner, C.; Parekh, B.; Walton, C.; Spanel, P.; Smith, D.; Evans, M. An Exploratory Comparative Study of Volatile Compounds in Exhaled Breath and Emitted by Skin Using Selected Ion Flow Tube Mass Spectrometry. *Rapid Commun. Mass Spectrom.* **2008**, *22*, 526–532. [CrossRef]

129. van Amsterdam, J.G.; Hollander, A.; Snelder, J.D.; Fischer, P.H.; van Loveren, H.; Vos, J.G.; Opperhuizen, A.; Steerenberg, P.A. The Effect of Air Pollution on Exhaled Nitric Oxide of Atopic and Nonatopic Subjects. *Nitric Oxide* **1999**, *3*, 492–495. [CrossRef]

130. Kushch, I.; Arendacká, B.; Štolc, S.; Mochalski, P.; Filipiak, W.; Schwarz, K.; Schwentner, L.; Schmid, A.; Dzien, A.; Lechleitner, M.; et al. Breath Isoprene—Aspects of Normal Physiology Related to Age, Gender and Cholesterol Profile as Determined in a Proton Transfer Reaction Mass Spectrometry Study. *Clin. Chem. Lab. Med.* **2008**, *46*, 1011–1018. [CrossRef]

131. Ishimaru, M.; Yamada, M.; Nakagawa, I.; Sugano, S. Analysis of Volatile Metabolites from Cultured Bacteria by Gas Chromatography/Atmospheric Pressure Chemical Ionization-Mass Spectrometry. *J. Breath Res.* **2008**, *2*, 037021. [CrossRef]

132. Smith, D.; Španěl, P. Selected Ion Flow Tube Mass Spectrometry (SIFT-MS) for on-Line Trace Gas Analysis. *Mass Spectrom. Rev.* **2005**, *24*, 661–700. [CrossRef]

133. von Basum, G.; Dahnke, H.; Halmer, D.; Hering, P.; Mürtz, M. Online Recording of Ethane Traces in Human Breath via Infrared Laser Spectroscopy. *J. Appl. Physiol.* **2003**, *95*, 2583–2590. [CrossRef] [PubMed]

134. Costello, B.P.J.D.L.; Ewen, R.J.; Ratcliffe, N.M. A Sensor System for Monitoring the Simple Gases Hydrogen, Carbon Monoxide, Hydrogen Sulfide, Ammonia and Ethanol in Exhaled Breath. *J. Breath Res.* **2008**, *2*, 037011. [CrossRef] [PubMed]

135. Gelperin, A.; Johnson, A.T.C. Nanotube-Based Sensor Arrays for Clinical Breath Analysis. *J. Breath Res.* **2008**, *2*, 037015. [CrossRef] [PubMed]

136. Burke, C.S.; Moore, J.P.; Wencel, D.; Maccraith, B.D. Development of a Compact Optical Sensor for Real-Time, Breath-by-Breath Detection of Oxygen. *J. Breath Res.* **2008**, *2*, 037012. [CrossRef] [PubMed]

137. Hibbard, T.; Killard, a. Breath Ammonia Analysis: Clinical Application and Measurement. *Crit. Rev. Anal. Chem.* **2011**, *41*, 21–35. [CrossRef]

138. Antus, B.; Horvath, I.; Barta, I. Assessment of Exhaled Nitric Oxide by a New Hand-Held Device. *Respir. Med.* **2010**, *104*, 1377–1380. [CrossRef]

139. Nishibori, M.; Shin, W.; Izu, N.; Itoh, T.; Matsubara, I. Sensing Performance of Thermoelectric Hydrogen Sensor for Breath Hydrogen Analysis. *Sens. Actuators B Chem.* **2009**, *137*, 524–528. [CrossRef]

140. Groves, W.A.; Achutan, C. Laboratory and Field Evaluation of a SAW Microsensor Array for Measuring Perchloroethylene in Breath. *J. Occup. Environ. Hyg.* **2004**, *1*, 779–788. [CrossRef]

141. Liao, J.Y.; Ho, K.C. A Study of Partially Irreversible Characteristics in a TTF-TCNQ Gas Sensing System. *Sens. Actuators B Chem.* **2008**, *130*, 343–350. [CrossRef]

142. Peng, G.; Tisch, U.; Haick, H. Detection of Nonpolar Molecules by Means of Carrier Scattering in Random Networks of Carbon Nanotubes: Toward Diagnosis of Diseases via Breath Samples. *Nano Lett.* **2009**, *9*, 1362–1368. [CrossRef]

143. Righettoni, M.; Tricoli, A.; Pratsinis, S.E. Si:WO_3 Sensors for Highly Selective Detection of Acetone for Easy Diagnosis of Diabetes by Breath Analysis. *Anal. Chem.* **2010**, *82*, 3581–3587. [CrossRef] [PubMed]

144. Davis, C.E.; Frank, M.; Mizaikoff, B.; Oser, H. Editorial the Future of Sensors and Instrumentation for Human Breath Analysis. *IEEE Sens. J.* **2010**, *10*, 3–6. [CrossRef]

145. Arakawa, T.; Wang, X.; Kajiro, T.; Miyajima, K.; Takeuchi, S.; Kudo, H.; Yano, K.; Mitsubayashi, K. A Direct Gaseous Ethanol Imaging System for Analysis of Alcohol Metabolism from Exhaled Breath. *Sens. Actuators B Chem.* **2013**, *186*, 27–33. [CrossRef]

146. Martin, J.D.M.; Romain, A.C. Building a Sensor Benchmark for E-Nose Based Lung Cancer Detection: Methodological Considerations. *Chemosensors* **2022**, *10*, 444. [CrossRef]

147. Mills, A.; Lepre, A.; Wild, L. Breath-by-Breath Measurement of Carbon Dioxide Using a Plastic Film Optical Sensor. *Sens. Actuators B Chem.* **1997**, *39*, 419–425. [CrossRef]

148. Fernández-Sánchez, J.F.; Cannas, R.; Spichiger, S.; Steiger, R.; Spichiger-Keller, U.E. Optical CO₂-Sensing Layers for Clinical Application Based on PH-Sensitive Indicators Incorporated into Nanoscopic Metal-Oxide Supports. *Sens. Actuators B Chem.* **2007**, *128*, 145–153. [CrossRef]

149. Sauerbrey, G. Verwendung von Schwingquarzen Zur Wägung Dünner Schichten Und Zur Mikrowägung. *Z. Phys.* **1959**, *155*, 206–222. [CrossRef]

150. Cui, D.; Cai, X.; Han, J.; He, Z.; Zhu, H.; Feng, G. Lipid LB Films for Room Temperature Ethanol Gas Assay. *Sens. Actuators B Chem.* **1997**, *45*, 229–232. [CrossRef]

151. Ito, J.; Nakamoto, T.; Uematsu, H. Discrimination of Halitosis Substance Using QCM Sensor Array and a Preconcentrator. *Sens. Actuators B Chem.* **2004**, *99*, 431–436. [CrossRef]

152. Pennazza, G.; Marchetti, E.; Santonico, M.; Mantini, G.; Mummolo, S.; Marzo, G.; Paolesse, R.; D'Amico, A.; Di Natale, C. Application of a Quartz Microbalance Based Gas Sensor Array for the Study of Halitosis. *J. Breath Res.* **2008**, *2*, 017009. [CrossRef]

153. Huang, H.; Zhou, J.; Chen, S.; Zeng, L.; Huang, Y. A Highly Sensitive QCM Sensor Coated with Ag+-ZSM-5 Film for Medical Diagnosis. *Sens. Actuators B Chem.* **2004**, *101*, 316–321. [CrossRef]

154. Brenet, S.; John-Herpin, A.; Gallat, F.X.; Musnier, B.; Buhot, A.; Herrier, C.; Rousselle, T.; Livache, T.; Hou, Y. Highly-Selective Optoelectronic Nose Based on Surface Plasmon Resonance Imaging for Sensing Volatile Organic Compounds. *Anal. Chem.* **2018**, *90*, 9879–9887. [CrossRef] [PubMed]

155. Boot, J.D.; de Ridder, L.; de Kam, M.L.; Calderon, C.; Mascelli, M.A.; Diamant, Z. Comparison of Exhaled Nitric Oxide Measurements between NIOX MINO® Electrochemical and Ecomedics Chemiluminescence Analyzer. *Respir. Med.* **2008**, *102*, 1667–1671. [CrossRef] [PubMed]

156. Vreman, H.J.; Stevenson, D.K.; Oh, W.; Fanaroff, A.A.; Wright, L.L.; Lemons, J.A.; Wright, E.; Shankaran, S.; Tyson, J.E.; Korones, S.B. Semiportable Electrochemical Instrument for Determining Carbon Monoxide in Breath. *Clin. Chem.* **1994**, *40*, 1927–1933. [CrossRef]

157. Kuban, P.; Berg, J.M.; Dasgupta, P.K. Durable Microfabricated High-Speed Humidity Sensors. *Anal. Chem.* **2004**, *76*, 2561–2567. [CrossRef]

158. Neri, G.; Bonavita, A.; Micali, G.; Donato, N. Design and Development of a Breath Acetone MOS Sensor for Ketogenic Diets Control. *IEEE Sens. J.* **2010**, *10*, 131–136. [CrossRef]

159. Marinelli, F.; Dell'Aquila, A.; Torsi, L.; Tey, J.; Suranna, G.P.; Mastrorilli, P.; Romanazzi, G.; Nobile, C.F.; Mhaisalkar, S.G.; Cioffi, N.; et al. An Organic Field Effect Transistor as a Selective NOx Sensor Operated at Room Temperature. *Sens. Actuators B Chem.* **2009**, *140*, 445–450. [CrossRef]

160. Sekiguchi, T.; Nakamura, M.; Kato, M.; Nishikawa, K.; Hokari, K.; Sugiyama, T.; Asaka, M. Immunological Helicobacter Pylori Urease Analyzer Based on Ion-Sensitive Field Effect Transistor. *Sens. Actuators B Chem.* **2000**, *67*, 265–269. [CrossRef]

161. Arshak, K.; Moore, E.; Lyons, G.M.; Harris, J.; Clifford, S. A Review of Gas Sensors Employed in Electronic Nose Applications. *Sens. Rev.* **2004**, *24*, 181–198. [CrossRef]

162. Eranna, G.; Joshi, B.C.; Runthala, D.P.; Gupta, R.P. Oxide Materials for Development of Integrated Gas Sensors—A Comprehensive Review. *Crit. Rev. Solid State Mater. Sci.* **2004**, *29*, 111–188. [CrossRef]

163. Wang, C.; Yin, L.; Zhang, L.; Xiang, D.; Gao, R. Metal Oxide Gas Sensors: Sensitivity and Influencing Factors. *Sensors* **2010**, *10*, 2088–2106. [CrossRef] [PubMed]

164. Schmid, W.; Bârsan, N.; Weimar, U. Sensing of Hydrocarbons with Tin Oxide Sensors: Possible Reaction Path as Revealed by Consumption Measurements. *Sens. Actuators B Chem.* **2003**, *89*, 232–236. [CrossRef]

165. Hamakawa, S.; Li, L.; Li, A.; Iglesia, E. Synthesis and Hydrogen Permeation Properties of Membranes Based on Dense SrCe0.95Yb0.05O3-a Thin Films. *Solid State Ion.* **2002**, *48*, 71–81. [CrossRef]

166. Dai, G. A Study of the Sensing Properties of Thin Film Sensor to Trimethylamine. *Sens. Actuators B Chem.* **1998**, *53*, 8–12. [CrossRef]

167. Espinosa, E.H.; Ionescu, R.; Chambon, B.; Bedis, G.; Sotter, E.; Bittencourt, C.; Felten, A.; Pireaux, J.J.; Correig, X.; Llobet, E. Hybrid Metal Oxide and Multiwall Carbon Nanotube Films for Low Temperature Gas Sensing. *Sens. Actuators B Chem.* **2007**, *127*, 137–142. [CrossRef]

168. Uma, S.; Shobana, M.K. Metal Oxide Semiconductor Gas Sensors in Clinical Diagnosis and Environmental Monitoring. *Sens. Actuators A Phys.* **2023**, *349*, 114044. [CrossRef]

169. Pour, G.B.; Behzadi, L.F. Influence of Oxide Film Surface Morphology and Thickness on the Properties of Gas Sensitive Nanostructure Sensor. *Indian J. Pure Appl. Phys.* **2019**, *57*, 743–749.

170. Fine, G.F.; Cavanagh, L.M.; Afonja, A.; Binions, R. Metal Oxide Semi-Conductor Gas Sensors in Environmental Monitoring. *Sensors* **2010**, *10*, 5469–5502. [CrossRef]

171. Feller, J.F. 6.10 Electrically Conductive Nanocomposites. In *Comprehensive Composite Materials II*; Beaumont, P.W.R., Zweben, C.H., Eds.; Elsevier: Amsterdam, The Netherlands, 2018; pp. 248–314.

172. Robert, C.; Feller, J.F.; Castro, M. Sensing Skin for Strain Monitoring Made of PC-CNT Conductive Polymer Nanocomposite Sprayed Layer by Layer. *ACS Appl. Mater. Interfaces* **2012**, *4*, 3508–3516. [CrossRef]

173. Lemartinel, A.; Castro, M.; Fouche, O.; De Luca, J.C.; Feller, J.F. Impact and Strain Monitoring in Glass Fiber Reinforced Epoxy Laminates with Embedded Quantum Resistive Sensors (QRSs). *Compos. Sci. Technol.* **2022**, *221*, 109352. [CrossRef]

174. Feller, J.F.; Castro, M.; Kumar, B. Polymer-Carbon Nanotube Conductive Nanocomposites for Sensing. In *Polymer-Carbon Nanotube Composites: Preparation, Properties & Applications*; McNally, T., Pötschke, P., Eds.; Woodhead Publishing: Cambridge, UK, 2011; pp. 760–803, ISBN 9781845697617.

175. Tripathi, K.M.; Sachan, A.; Castro, M.; Choudhary, V.; Sonkar, S.K.; Feller, J.F. Green Carbon Nanostructured Quantum Resistive Sensors to Detect Volatile Biomarkers. *Sustain. Mater. Technol.* **2018**, *16*, 1–11. [CrossRef]

176. Duarte, L.; Nag, S.; Castro, M.; Zaborova, E.; Ménand, M.; Sollogoub, M.; Bennevault, V.; Feller, J.F.; Guégan, P. Chemical Sensors Based on New Polyamides Biobased on (Z) Octadec-9-Enedioic Acid and β-Cyclodextrin. *Macromol. Chem. Phys.* **2016**, *217*, 1620–1628. [CrossRef]

177. Castro, M.; Lu, J.; Bruzaud, S.; Kumar, B.; Feller, J.F. Carbon Nanotubes/Poly(ε-Caprolactone) Composite Vapour Sensors. *Carbon* **2009**, *47*, 1930–1942. [CrossRef]

178. Wang, J.; Musameh, M. Carbon Nanotube/Teflon Composite Electrochemical Sensors and Biosensors. *Anal. Chem.* **2003**, *75*, 2075–2079. [CrossRef] [PubMed]

179. Radushkevich, L.V.; Lukyanovich, V.M. About the Structure of Carbon Formed by Thermal Decomposition of Carbon Monoxide on Iron Substrate. *J. Phys. Chem. (Mosc.)* **1952**, *26*, 88–95.

180. Iijima, S. Helical Microtubules of Graphitic Carbon. *Nature* **1991**, *354*, 56–58. [CrossRef]

181. Meyyappan, M. *Carbon Nanotubes: Science and Applications*; CRC Press: Boca Raton, FL, USA, 2005; ISBN 0849321115.

182. Saito, R.; Fujita, M.; Dresselhaus, G.; Dresselhaus, M.S. Electronic Structure of Chiral Graphene Tubules. *Appl. Phys. Lett.* **1992**, *60*, 2204–2206. [CrossRef]

183. Sinha, N.; Ma, J.; Yeow, J.T.W. Carbon Nanotube-Based Sensors. *J. Nanosci. Nanotechnol.* **2006**, *6*, 573–590. [CrossRef]

184. Llobet, E. Gas Sensors Using Carbon Nanomaterials: A Review. *Sens. Actuators B Chem.* **2013**, *179*, 32–45. [CrossRef]

185. Kroto, H.W. The Stability of the Fullerenes Cn, with n = 24, 28, 32, 36, 50, 60 and 70. *Nature* **1987**, *329*, 529–531. [CrossRef]

186. Di Crescenzo, A.; Ettorre, V.; Fontana, A. Non-Covalent and Reversible Functionalization of Carbon Nanotubes. *Beilstein J. Nanotechnol.* **2014**, *5*, 1675–1690. [CrossRef] [PubMed]

187. Hirsch, A. Functionalization of Single-Walled Carbon Nanotubes. *Angew. Chem. Int. Ed.* **2002**, *41*, 1853–1859. [CrossRef]

188. Niyogi, S.; Hamon, M.A.; Hu, H.; Zhao, B.; Bhowmik, P.; Sen, R.; Itkis, M.E.; Haddon, R.C. Chemistry of Single-Walled Carbon Nanotubes. *Acc. Chem. Res.* **2002**, *35*, 1105–1113. [CrossRef] [PubMed]

189. Sin, M.L.Y.; Chow, G.C.T.; Wong, G.M.K.; Li, W.J.; Leong, P.H.W.; Wong, K.W. Ultralow-Power Alcohol Vapor Sensors Using Chemically Functionalized Multiwalled Carbon Nanotubes. *IEEE Trans. Nanotechnol.* **2007**, *6*, 571–577. [CrossRef]

190. Norizan, M.N.; Moklis, M.H.; Ngah Demon, S.Z.; Halim, N.A.; Samsuri, A.; Mohamad, I.S.; Knight, V.F.; Abdullah, N. Carbon Nanotubes: Functionalisation and Their Application in Chemical Sensors. *RSC Adv.* **2020**, *10*, 43704–43732. [CrossRef]

191. Nag, S.; Sachan, A.; Castro, M.; Choudhary, V.; Feller, J.F. Spray Layer-by-Layer Assembly of POSS Functionalized CNT Quantum Chemo-Resistive Sensors with Tuneable Selectivity and Ppm Resolution to VOC Biomarkers. *Sens. Actuators B Chem.* **2016**, *222*, 362–373. [CrossRef]

192. Kong, J.; Chapline, M.G.; Dai, H. Functionalized Carbon Nanotubes for Molecular Hydrogen Sensors. *Adv. Mater.* **2001**, *13*, 1384–1386. [CrossRef]

193. Sayago, I.; Terrado, E.; Lafuente, E.; Horrillo, M.C.; Maser, W.K.; Benito, A.M.; Navarro, R.; Urriolabeitia, E.P.; Martinez, M.T.; Gutierrez, J. Hydrogen Sensors Based on Carbon Nanotubes Thin Films. *Synth. Met.* **2005**, *148*, 15–19. [CrossRef]

194. Yun, Y.; Dong, Z.; Shanov, V.; Heineman, W.R.; Halsall, H.B.; Bhattacharya, A.; Conforti, L.; Narayan, R.K.; Ball, W.S.; Schulz, M.J. Nanotube Electrodes and Biosensors. *Nano Today* **2007**, *2*, 30–37. [CrossRef]

195. Sachan, A.; Castro, M.; Choudhary, V.; Feller, J.F. Influence of Water Molecules on the Detection of Volatile Organic Compounds (VOC) Cancer Biomarkers by Nanocomposite Quantum Resistive Vapour Sensors VQRS. *Chemosensors* **2018**, *6*, 64. [CrossRef]

196. Tung, T.T.; Castro, M.; Kim, T.Y.; Suh, K.S.; Feller, J.F. High Stability Silver Nanoparticles–Graphene/Poly(Ionic Liquid)-Based Chemoresistive Sensors for Volatile Organic Compounds' Detection. *Anal. Bioanal. Chem.* **2014**, *406*, 3995–4004. [CrossRef] [PubMed]

197. Nasiri, N.; Clarke, C. Nanostructured Chemiresistive Gas Sensors for Medical Applications. *Sensors* **2019**, *19*, 462. [CrossRef] [PubMed]

198. Tung, T.T.; Castro, M.; Pillin, I.; Kim, T.Y.; Suh, K.S.; Feller, J.F. Graphene—Fe_3O_4/PIL–PEDOT for the Design of Sensitive and Stable Quantum Chemo-Resistive VOC Sensors. *Carbon* **2014**, *74*, 104–112. [CrossRef]

199. Nag, S.; Castro, M.; Choudhary, V.; Feller, J.-F. Boosting Selectivity and Sensitivity to Biomarkers of Quantum Resistive Vapour Sensors Used for Volatolomics with Nanoarchitectured Carbon Nanotubes or Graphene Platelets Connected by Fullerene Junctions. *Chemosensors* **2021**, *9*, 66. [CrossRef]

200. Jian, Y.; Hu, W.; Zhao, Z.; Cheng, P.; Haick, H.; Yao, M.; Wu, W. Gas Sensors Based on Chemi-Resistive Hybrid Functional Nanomaterials. *Nanomicro Lett.* **2020**, *12*, 71. [CrossRef]

201. Zhang, L.; Khan, K.; Zou, J.; Zhang, H.; Li, Y. Recent Advances in Emerging 2D Material-based Gas Sensors: Potential in Disease Diagnosis. *Adv. Mater. Interfaces* **2019**, *6*, 1901329. [CrossRef]

202. Tung, T.T.; Tran, M.T.; Feller, J.F.; Castro, M.; Van Ngo, T.; Hassan, K.; Nine, M.J.; Losic, D. Graphene and Metal Organic Frameworks (MOFs) Hybridization for Tunable Chemoresistive Sensors for Detection of Volatile Organic Compounds (VOCs) Biomarkers. *Carbon* **2020**, *159*, 333–344. [CrossRef]

203. Mishra, S.K.; Tripathi, S.N.; Choudhary, V.; Gupta, B.D. SPR Based Fiber Optic Ammonia Gas Sensor Utilizing Nanocomposite Film of PMMA / Reduced Graphene Oxide Prepared by in Situ Polymerization. *Sens. Actuators B Chem.* **2014**, *199*, 190–200. [CrossRef]

204. Bai, H.; Xu, Y.; Zhao, L.; Li, C.; Shi, G. Non-Covalent Functionalization of Graphene Sheets by Sulfonated Polyaniline. *Chem. Commun.* **2009**, *4*, 1667–1669. [CrossRef]

205. Tung, T.T.; Castro, M.; Feller, J.F.; Kim, T.Y.; Suh, K.S. Hybrid Film of Chemically Modified Graphene and Vapor-Phase-Polymerized PEDOT for Electronic Nose Applications. *Org. Electron.* **2013**, *14*, 2789–2794. [CrossRef]

206. Xiang, C.; Jiang, D.; Zou, Y.; Chu, H.; Qiu, S.; Zhang, H.; Xu, F.; Sun, L.; Zheng, L. Ammonia Sensor Based on Polypyrrole–Graphene Nanocomposite Decorated with Titania Nanoparticles. *Ceram. Int.* **2015**, *41*, 6432–6438. [CrossRef]

207. Dariyal, P.; Sharma, S.; Chauhan, G.S.; Singh, B.P.; Dhakate, S.R. Recent Trends in Gas Sensing via Carbon Nanomaterials: Outlook and Challenges. *Nanoscale Adv.* **2021**, *3*, 6514–6544. [CrossRef] [PubMed]

208. Shurmer, H.V.; Gardner, J.W. Odour Discrimination with an Electronic Nose. *Sens. Actuators B Chem.* **1992**, *8*, 1–11. [CrossRef]

209. Gardner, J.W.; Shin, H.W.; Hines, E.L. An Electronic Nose System to Diagnose Illness. *Sens. Actuators B Chem.* **2000**, *70*, 19–24. [CrossRef]

210. Gao, T.; Woodka, M.D.; Brunschwig, B.S.; Lewis, N.S. Chemiresistors for Array-Based Vapor Sensing Using Composites of Carbon Black with Low Volatility Organic Molecules. *Chem. Mater.* **2006**, *18*, 5193–5202. [CrossRef]

211. D'Amico, A.; Pennazza, G.; Santonico, M.; Martinelli, E.; Roscioni, C.; Galluccio, G.; Paolesse, R.; Di Natale, C. An Investigation on Electronic Nose Diagnosis of Lung Cancer. *Lung Cancer* **2010**, *68*, 170–176. [CrossRef]

212. D'Amico, A.; Di Natale, C.; Sarro, P.M. Ingredients for Sensors Science. *Sens. Actuators B Chem.* **2015**, *207*, 1060–1068. [CrossRef]

213. Ziyatdinov, A.; Fernández Diaz, E.; Chaudry, A.; Marco, S.; Persaud, K.; Perera, A. A Software Tool for Large-Scale Synthetic Experiments Based on Polymeric Sensor Arrays. *Sens. Actuators B Chem.* **2013**, *177*, 596–604. [CrossRef]

214. Hakim, M.; Broza, Y.Y.; Barash, O.; Peled, N.; Phillips, M.; Amann, A.; Haick, H. Volatile Organic Compounds of Lung Cancer and Possible Biochemical Pathways. *Chem. Rev.* **2012**, *112*, 5949–5966. [CrossRef]

215. Bachar, N.; Mintz, L.; Zilberman, Y.; Ionescu, R.; Feng, X.; Müllen, K.; Haick, H. Polycyclic Aromatic Hydrocarbon for the Detection of Nonpolar Analytes under Counteracting Humidity Conditions. *ACS Appl. Mater. Interfaces* **2012**, *4*, 4960–4965. [CrossRef]

216. Peng, G.; Tisch, U.; Adams, O.; Hakim, M.; Shehada, N.; Broza, Y.Y.; Billan, S.; Abdah-Bortnyak, R.; Kuten, A.; Haick, H. Diagnosing Lung Cancer in Exhaled Breath Using Gold Nanoparticles. *Nat. Nanotechnol.* **2009**, *4*, 669–673. [CrossRef] [PubMed]

217. Nakhleh, M.K.; Amal, H.; Jeries, R.; Broza, Y.Y.; Aboud, M.; Gharra, A.; Ivgi, H.; Khatib, S.; Badarneh, S.; Har-Shai, L.; et al. Diagnosis and Classification of 17 Diseases from 1404 Subjects via Pattern Analysis of Exhaled Molecules. *ACS Nano* **2017**, *11*, 112–125. [CrossRef] [PubMed]

218. Hurot, C.; Scaramozzino, N.; Buhot, A.; Hou, Y. Bio-Inspired Strategies for Improving the Selectivity and Sensitivity of Artificial Noses: A Review. *Sensors* **2020**, *20*, 1803. [CrossRef] [PubMed]

219. Wasilewski, T.; Gębicki, J.; Kamysz, W. Advances in Olfaction-Inspired Biomaterials Applied to Bioelectronic Noses. *Sens. Actuators B Chem.* **2018**, *257*, 511–537. [CrossRef]

220. Spencer, T.L.; Lavrik, N.; Hu, D.L. Synthetic Moth Antennae Fabricated as Preconcentrator for Odor Collection. In Proceedings of the 2017 ISOCS/IEEE International Symposium on Olfaction and Electronic Nose (ISOEN), Montreal, QC, Canada, 28–31 May 2017; pp. 1–3.

221. Raman, B.; Sun, P.A.; Gutierrez-Galvez, A.; Gutierrez-Osuna, R. Processing of Chemical Sensor Arrays with a Biologically Inspired Model of Olfactory Coding. *IEEE Trans. Neural Netw.* **2006**, *17*, 1015–1024. [CrossRef]

222. Hervé-Bazin, B.; Ambroise, D.; Brémer, D.; Binet, S.; Courtois, B.; Fubini, B.; Gensdarmes, F.; Jaurand, M.C.; Lacroix, G.; Lafon, D.; et al. *Les Nanoparticules: Un Enjeu Majeur Pour La Santé Au Travail?* Hervé-Bazin, B., Ed.; EDP Science: Les Ulis, France, 2007.

223. Li, N.; Sioutas, C.; Cho, A.; Schmitz, D.; Misra, C.; Sempf, J.; Wang, M.; Oberley, T.; Froines, J.; Nel, A. Ultrafine Particulate Pollutants Induce Oxidative Stress and Mitochondrial Damage. *Environ. Health Perspect.* **2002**, *111*, 455–460. [CrossRef]

224. Geiser, M.; Rothen-Rutishauser, B.; Kapp, N.; Schürch, S.; Kreyling, W.; Schulz, H.; Semmler, M.; Hof, V.I.; Heyder, J.; Gehr, P. Ultrafine Particles Cross Cellular Membranes by Nonphagocytic Mechanisms in Lungs and in Cultured Cells. *Environ. Health Perspect.* **2005**, *113*, 1555–1560. [CrossRef]

225. Duarte, K.; Justino, C.I.L.; Freitas, A.C.; Duarte, A.C.; Rocha-Santos, T.A.P. Direct-Reading Methods for Analysis of Volatile Organic Compounds and Nanoparticles in Workplace Air. *Trends Anal. Chem.* **2013**, *53*, 21–32. [CrossRef]

226. Ma-Hock, L.; Strauss, V.; Treumann, S.; Küttler, K.; Wohlleben, W.; Hofmann, T.; Gröters, S.; Wiench, K.; van Ravenzwaay, B.; Landsiedel, R. Comparative Inhalation Toxicity of Multi-Wall Carbon Nanotubes, Graphene, Graphite Nanoplatelets and Low Surface Carbon Black. *Part. Fibre Toxicol.* **2013**, *10*, 23. [CrossRef]

227. Guo, N.L.; Wan, Y.; Denvir, J.; Porter, D.W.; Pacurari, M.; Wolfarth, M.G.; Castranova, V.; Qian, Y.; Babb, M.; Cancer, R. Multi-Walled Carbon Nanotube-Induced Gene Signatures in the Mouse Lung: Potential Predictive Value for Human Lung Cancer Risk and Prognosis. *J. Toxicol. Environ. Health A* **2012**, *75*, 1129–1153. [CrossRef]

228. Bellucci, S. Carbon Nanotubes Toxicity. In *Nanoparticles and Nanodevices in Biological Applications*; Springer: Berlin/Heidelberg, Germany, 2009; pp. 47–67.

229. Zhao, X.; Liu, R. Recent Progress and Perspectives on the Toxicity of Carbon Nanotubes at Organism, Organ, Cell, and Biomacromolecule Levels. *Environ. Int.* **2012**, *40*, 244–255. [CrossRef] [PubMed]

230. Ou, L.; Song, B.; Liang, H.; Liu, J.; Feng, X.; Deng, B.; Sun, T.; Shao, L. Toxicity of Graphene-Family Nanoparticles: A General Review of the Origins and Mechanisms. *Part. Fibre Toxicol.* **2016**, *13*, 57. [CrossRef] [PubMed]

231. Mytych, J.; Maciej, W. Nanoparticle Technology as a Double-Edged Sword: Cytotoxic, Genotoxic and Epigenetic Effects on Living Cells. *J. Biomater. Nanobiotechnol.* **2013**, *4*, 53–63. [CrossRef]

232. Wang, K.; Ruan, J.; Song, H.; Zhang, J.; Wo, Y.; Guo, S.; Cui, D. Biocompatibility of Graphene Oxide. *Nanoscale Res. Lett.* **2011**, *6*, 8. [CrossRef] [PubMed]

233. Buck, L.; Axel, R. A Novel Multigene Family May Encode Odorant Receptors: A Molecular Basis for Odor Recognition. *Cell* **1991**, *65*, 175–187. [CrossRef]

234. Wang, X.; Zhou, Y.; Zhao, Z.; Feng, X.; Wang, Z.; Jiao, M. Advanced Algorithms for Low Dimensional Metal Oxides-Based Electronic Nose Application: A Review. *Crystals* **2023**, *13*, 615. [CrossRef]

235. Wilson, A.D.; Baietto, M. Applications and Advances in Electronic-Nose Technologies. *Sensors* **2009**, *9*, 5099–5148. [CrossRef]

236. Russo, D.V.; Burek, M.J.; Iutzi, R.M.; Mracek, J.A.; Hesjedal, T. Development of an Electronic Nose Sensing Platform for Undergraduate Education in Nanotechnology. *Eur. J. Phys.* **2011**, *32*, 675. [CrossRef]

237. Burl, M.C.; Doleman, B.J.; Schaffer, A.; Lewis, N.S. Assessing the Ability to Predict Human Percepts of Odor Quality from the Detector Responses of a Conducting Polymer Composite-Based Electronic Nose. *Sens. Actuators B Chem.* **2001**, *72*, 149–159. [CrossRef]

238. Lu, A. Piezoelectric Phenomenon of Fullerene-Graphene Bonded Structure. *J. Nanomater.* **2014**, *2014*, 943013. [CrossRef]

239. Tran, M.T.; Kumar, A.; Sachan, A.; Castro, M.; Allegre, W.; Feller, J.F. Emerging strategies based on sensors for chronic wound monitoring and management. *Chemosensors* **2022**, *10*, 311. [CrossRef]

240. Feller, J.F.; Grohens, Y. Electrical Response of Poly(Styrene)/Carbon Black Conductive Polymer Composites (CPC) to Methanol, Toluene, Chloroform and Styrene Vapors as a Function of Filler Nature and Matrix Tacticity. *Synth. Met.* **2005**, *154*, 193–196. [CrossRef]

241. Nagle, H.T.; Gutierrez-Osuna, R.; Schiffman, S.S. The How and Why of Electronic Noses. *IEEE Spectr.* **1998**, *35*, 22–31. [CrossRef]

242. Persaud, K.; Dodd, G. Analysis of Discrimination Mechanisms in the Mammalian Olfactory System Using a Model Nose. *Nature* **1982**, *299*, 352–355. [CrossRef]

243. Konvalina, G.; Haick, H. Sensors for Breath Testing: From Nanomaterials to Comprehensive Disease Detection. *Acc. Chem. Res.* **2014**, *47*, 66–76. [CrossRef]

244. Scott, S.M.; James, D.; Ali, Z. Data Analysis for Electronic Nose Systems. *Microchim. Acta* **2006**, *156*, 183–207. [CrossRef]

245. Ferreiro-González, M.; Barbero, G.F.; Palma, M.; Ayuso, J.; Álvarez, J.A.; Barroso, C.G. Determination of Ignitable Liquids in Fire Debris: Direct Analysis by Electronic Nose. *Sensors* **2016**, *16*, 695. [CrossRef]

246. Mertens, B.; Thompson, M.; Fearn, T. Principal Component Outlier Detection and SIMCA: A Synthesis. *Analyst* **1994**, *119*, 2777–2784. [CrossRef]

247. Amari, A.; El Bari, N.; Bouchikhi, B. Electronic Nose for Anchovy Freshness Monitoring Based on Sensor Array and Pattern Recognition Methods: Principal Components Analysis, Linear Discriminant Analysis and Support Vector Machine. *Int. J. Comput.* **2014**, *6*, 61–67. [CrossRef]

248. Hai, Z.; Wang, J. Electronic Nose and Data Analysis for Detection of Maize Oil Adulteration in Sesame Oil. *Sens. Actuators B Chem.* **2006**, *119*, 449–455. [CrossRef]

249. Campbell, M.G.; Liu, S.F.; Swager, T.M.; Dincă, M. Chemiresistive Sensor Arrays from Conductive 2D Metal-Organic Frameworks. *J. Am. Chem. Soc.* **2015**, *137*, 13780–13783. [CrossRef] [PubMed]

250. Fisher, R.A. The Statistical Utilization of Multiple Measurements. *Ann. Eugen.* **1938**, *8*, 376–386. [CrossRef]

251. Fisher, R.A. The Use of Multiple Measurements in Taxonomic Problems. *Ann. Eugen.* **1936**, *7*, 179–188. [CrossRef]

252. Qiu, S.; Wang, J.; Gao, L. Discrimination and Characterization of Strawberry Juice Based on Electronic Nose and Tongue: Comparison of Different Juice Processing Approaches by LDA, PLSR, RF, and SVM. *J. Agric. Food Chem.* **2014**, *62*, 6426–6434. [CrossRef] [PubMed]

253. Bishop, C.M. Neural Networks for Pattern Recognition. *J. Am. Stat. Assoc.* **1995**, *92*, 482. [CrossRef]

254. Tisan, A.; Chin, J. An End-User Platform for FPGA-Based Design and Rapid Prototyping of Feedforward Artificial Neural Networks With On-Chip Backpropagation Learning. *IEEE Trans. Ind. Inf.* **2016**, *12*, 1124–1133. [CrossRef]

255. Pardo, M.; Sberveglieri, G. Remarks on the Use of Multilayer Perceptrons for the Analysis of Chemical Sensor Array Data. *Sens. J. IEEE* **2004**, *4*, 355–363. [CrossRef]

256. Uyanık, T.; Yalman, Y.; Kalenderli, Ö.; Arslanoğlu, Y.; Terriche, Y.; Su, C.L.; Guerrero, J.M. Data-Driven Approach for Estimating Power and Fuel Consumption of Ship: A Case of Container Vessel. *Mathematics* **2022**, *10*, 4167. [CrossRef]

257. Gardner, J.W.; Boilot, P.; Hines, E.L. Enhancing Electronic Nose Performance by Sensor Selection Using a New Integer-Based Genetic Algorithm Approach. *Sens. Actuators B Chem.* **2005**, *106*, 114–121. [CrossRef]

258. Yan, J.; Guo, X.; Duan, S.; Jia, P.; Wang, L.; Peng, C.; Zhang, S. Electronic Nose Feature Extraction Methods: A Review. *Sensors* **2015**, *15*, 27804–27831. [CrossRef]

259. Rath, R.J.; Farajikhah, S.; Oveissi, F.; Dehghani, F.; Naficy, S. Chemiresistive Sensor Arrays for Gas/Volatile Organic Compounds Monitoring: A Review. *Adv. Eng. Mater.* **2022**, *25*, 2200830. [CrossRef]

260. Schroeder, V.; Evans, E.D.; Wu, Y.C.M.; Voll, C.C.A.; McDonald, B.R.; Savagatrup, S.; Swager, T.M. Chemiresistive Sensor Array and Machine Learning Classification of Food. *ACS Sens.* **2019**, *4*, 2101–2108. [CrossRef] [PubMed]

261. Aguilera, T.; Lozano, J.; Paredes, J.A.; Álvarez, F.J.; Suárez, J.I. Electronic Nose Based on Independent Component Analysis Combined with Partial Least Squares and Artificial Neural Networks for Wine Prediction. *Sensors* **2012**, *12*, 8055–8072. [CrossRef] [PubMed]

262. Camardo Leggieri, M.; Mazzoni, M.; Fodil, S.; Moschini, M.; Bertuzzi, T.; Prandini, A.; Battilani, P. An Electronic Nose Supported by an Artificial Neural Network for the Rapid Detection of Aflatoxin B1 and Fumonisins in Maize. *Food Control* **2021**, *123*, 107722. [CrossRef]

263. Tan, J.; Kerr, W.L. Determining Degree of Roasting in Cocoa Beans by Artificial Neural Network (ANN)-based Electronic Nose System and Gas Chromatography/Mass Spectrometry (GC/MS). *J. Sci. Food Agric.* **2018**, *98*, 3851–3859. [CrossRef]

264. Panigrahi, S.; Balasubramanian, S.; Gu, H.; Logue, C.; Marchello, M. Neural-Network-Integrated Electronic Nose System for Identification of Spoiled Beef. *LWT* **2006**, *39*, 135–145. [CrossRef]

265. Zhang, D.; Liu, J.; Jiang, C.; Liu, A.; Xia, B. Quantitative Detection of Formaldehyde and Ammonia Gas via Metal Oxide-Modified Graphene-Based Sensor Array Combining with Neural Network Model. *Sens. Actuators B Chem.* **2017**, *240*, 55–65. [CrossRef]

266. Aghilinategh, N.; Dalvand, M.J.; Anvar, A. Detection of Ripeness Grades of Berries Using an Electronic Nose. *Food Sci. Nutr.* **2020**, *8*, 4919–4928. [CrossRef]

267. Zakaria, A.; Shakaff, A.Y.M.; Masnan, M.J.; Ahmad, M.N.; Adom, A.H.; Jaafar, M.N.; Ghani, S.A.; Abdullah, A.H.; Aziz, A.H.A.; Kamarudin, L.M.; et al. A Biomimetic Sensor for the Classification of Honeys of Different Floral Origin and the Detection of Adulteration. *Sensors* **2011**, *11*, 7799–7822. [CrossRef]

268. Machado, R.F.; Laskowski, D.; Deffenderfer, O.; Burch, T.; Zheng, S.; Mazzone, P.J.; Mekhail, T.; Jennings, C.; Stoller, J.K.; Pyle, J.; et al. Detection of Lung Cancer by Sensor Array Analyses of Exhaled Breath. *Am. J. Respir. Crit. Care Med.* **2005**, *171*, 1286–1291. [CrossRef]

269. Chen, X.; Cao, M.; Li, Y.; Hu, W.; Wang, P.; Ying, K.; Pan, H. A Study of an Electronic Nose for Detection of Lung Cancer Based on a Virtual SAW Gas Sensors Array and Imaging Recognition Method. *Meas. Sci. Technol.* **2005**, *16*, 1535–1546. [CrossRef]

270. Nurputra, D.K.; Kusumaatmaja, A.; Hakim, M.S.; Hidayat, S.N.; Julian, T.; Sumanto, B.; Mahendradhata, Y.; Saktiawati, A.M.I.; Wasisto, H.S.; Triyana, K. Fast and Noninvasive Electronic Nose for Sniffing out COVID-19 Based on Exhaled Breath-Print Recognition. *NPJ Digit. Med.* **2022**, *5*, 115. [CrossRef] [PubMed]

271. Kwiatkowski, A.; Borys, S.; Sikorska, K.; Drozdowska, K.; Smulko, J.M. Clinical Studies of Detecting COVID-19 from Exhaled Breath with Electronic Nose. *Sci. Rep.* **2022**, *12*, 1–9. [CrossRef] [PubMed]

272. Li, Y.; Wei, X.; Zhou, Y.; Wang, J.; You, R. Research Progress of Electronic Nose Technology in Exhaled Breath Disease Analysis. *Microsyst. Nanoeng.* **2023**, *9*, 129. [CrossRef]

273. Bochenkov, V.E.; Sergeev, G.B. Sensitivity, Selectivity, and Stability of Gas-Sensitive Metal-Oxide Nanostructures. In *Metal Oxide Nanostructures & Their Applications*; American Scientific Publishers: Santa Clarita, CA, USA, 2010; Volume 3, pp. 31–52, ISBN 1588831760.

274. Persaud, K.; Khaffaf, S.M.; Payne, J.S.; Pisanelli, A.M.; Lee, D.H.; Byun, H.G. Sensor Array Techniques for Mimicking the Mammalian Olfactory System. *Sens. Actuators B* **1996**, *35*, 267–273. [CrossRef]

275. Shurmer, H.V.; Gardner, J.W.; Corcoran, P. Intelligent Vapour Discrimination Using a Composite 12-Element Sensor Array. *Sens. Actuators B Chem.* **1990**, *1*, 256–260. [CrossRef]

276. Wilson, A.D. Review of Electronic-Nose Technologies and Algorithms to Detect Hazardous Chemicals in the Environment. *Procedia Technol.* **2012**, *1*, 453–463. [CrossRef]

277. Wilson, A.D. Recent applications of electronic-nose technologies for the noninvasive early diagnosis of gastrointestinal diseases. *Proceedings* **2018**, *2*, 147. [CrossRef]

278. Wilson, A.D. Applications of Electronic-Nose Technologies for Noninvasive Early Detection of Plant, Animal and Human Diseases. *Chemosensors* **2018**, *6*, 45. [CrossRef]

279. Ryan, M.A.; Zhou, H.; Buehler, M.G.; Manatt, K.S.; Mowrey, V.S.; Jackson, S.P.; Kisor, A.K.; Shevade, A.V.; Homer, M.L. Monitoring Space Shuttle Air Quality Using the Jet Propulsion Laboratory Electronic Nose. *IEEE Sens. J.* **2004**, *4*, 337–347. [CrossRef]

280. Covington, J.; Westenbrink, E.; Ouaret, N.; Harbord, R.; Bailey, C.; O'Connell, N.; Cullis, J.; Williams, N.; Nwokolo, C.; Bardhan, K.; et al. Application of a Novel Tool for Diagnosing Bile Acid Diarrhoea. *Sensors* **2013**, *13*, 11899–11912. [CrossRef] [PubMed]

281. Shuster, G.; Gallimidi, Z.; Heyman Reiss, A.; Dovgolevsky, E.; Billan, S.; Abdah-Bortnyak, R.; Kuten, A.; Engel, A.; Shiban, A.; Tisch, U.; et al. Classification of breast cancer precursors through exhaled. *Breast Cancer Res. Treat.* **2011**, *126*, 791–796. [CrossRef] [PubMed]

282. Haick, H.; Broza, Y.Y.; Mochalski, P.; Ruzsanyi, V.; Amann, A. Assessment, Origin, and Implementation of Breath Volatile Cancer Markers. *Chem. Soc. Rev.* **2014**, *43*, 1423–1449. [CrossRef] [PubMed]

283. Du, D.; Wang, J.; Wang, B.; Zhu, L.; Hong, X. Ripeness Prediction of Post Harvest Kiwifruit Using a MOS E-Nose Combined with Chemometrics. *Sensors* **2019**, *19*, 419. [CrossRef]

284. Miller, T.C.; Morgera, S.D.; Saddow, S.E.; Takshi, A.; Mullarkey, M.; Palm, M. Neurological Connections and Endogenous Biochemistry—Potentially Useful in Electronic-Nose Diagnostics for Coronavirus Diseases. *Neurosciences* **2021**, *8*, 284. [CrossRef]

285. Bikov, A.; Lázár, Z.; Horvath, I. Established Methodological Issues in Electronic Nose Research: How Far Are We from Using These Instruments in Clinical Settings of Breath Analysis? *J. Breath Res.* **2015**, *9*, 034001. [CrossRef]

286. Dragonieri, S.; van der Schee, M.P.; Massaro, T.; Schiavulli, N.; Brinkman, P.; Pinca, A.; Carratú, P.; Spanevello, A.; Resta, O.; Musti, M.; et al. An Electronic Nose Distinguishes Exhaled Breath of Patients with Malignant Pleural Mesothelioma from Controls. *Lung Cancer* **2012**, *75*, 326–331. [CrossRef]

287. Chapman, E.A.; Thomas, P.S.; Stone, E.; Lewis, C.; Yates, D.H. A Breath Test for Malignant Mesothelioma Using an Electronic Nose. *Eur. Respir. J.* **2012**, *40*, 448–454. [CrossRef]

288. Dragonieri, S.; Schot, R.; Mertens, B.J.A.; Le Cessie, S.; Gauw, S.A.; Spanevello, A.; Resta, O.; Willard, N.P.; Vink, T.J.; Rabe, K.F.; et al. An Electronic Nose in the Discrimination of Patients with Asthma and Controls. *J. Allergy Clin. Immunol.* **2007**, *120*, 856–862. [CrossRef]

289. Sensigent Technical Characteristics of the Cyranose 320 Electronic Nose. Available online: https://www.sensigent.com/cyranose-320.html (accessed on 7 January 2025).

290. Montuschi, P.; Santonico, M.; Mondino, C.; Pennazza, G.; Maritini, G.; Martinelli, E.; Capuano, R.; Ciabattoni, G.; Paolesse, R.; Di Natale, C.; et al. Diagnostic Performance of an Electronic Nose, Fractional Exhaled Nitric Oxide, and Lung Function Testing in Asthma. *Chest* **2010**, *137*, 790–796. [CrossRef]

291. Kaloumenou, M.; Skotadis, E.; Lagopati, N.; Efstathopoulos, E.; Tsoukalas, D. Breath Analysis: A Promising Tool for Disease Diagnosis—The Role of Sensors. *Sensors* **2022**, *22*, 1238. [CrossRef] [PubMed]

292. Di Natale, C.; Macagnano, A.; Martinelli, E.; Paolesse, R.; D'Arcangelo, G.; Roscioni, C.; Finazzi-Agrò, A.; D'Amico, A. Lung Cancer Identification by the Analysis of Breath by Means of an Array of Non-Selective Gas Sensors. *Biosens. Bioelectron.* **2003**, *18*, 1209–1218. [CrossRef] [PubMed]

293. Mazzone, P.J.; Hammel, J.; Dweik, R.; Na, J.; Czich, C.; Laskowski, D.; Mekhail, T. Diagnosis of Lung Cancer by the Analysis of Exhaled Breath with a Colorimetric Sensor Array. *Thorax* **2007**, *62*, 565–568. [CrossRef]

294. Mazzone, P.J.; Wang, X.-F.; Xu, Y.; Mekhail, T.; Beukemann, M.C.; Na, J.; Kemling, J.W.; Suslick, K.S.; Sasidhar, M. Exhaled Breath Analysis with a Colorimetric Sensor Array for the Identification and Characterization of Lung Cancer. *J. Thorac. Oncol.* **2012**, *7*, 137–142. [CrossRef]

295. Pavlou, A.K.; Magan, N.; Jones, J.M.; Brown, J.; Klatser, P.; Turner, A.P.F. Detection of Mycobacterium Tuberculosis (TB) in Vitro and in Situ Using an Electronic Nose in Combination with a Neural Network System. *Biosens. Bioelectron.* **2004**, *20*, 538–544. [CrossRef]

296. Fend, R.; Kolk, A.H.J.; Bessant, C.; Buijtels, P.; Klatser, P.R.; Woodman, A.C. Prospects for Clinical Application of Electronic-Nose Technology to Early Detection of Mycobacterium Tuberculosis in Culture and Sputum. *J. Clin. Microbiol.* **2006**, *44*, 2039–2045. [CrossRef]

297. Phillips, M.; Basa-Dalay, V.; Blais, J.; Bothamley, G.; Chaturvedi, A.; Modi, K.D.; Pandya, M.; Natividad, M.P.R.; Patel, U.; Ramraje, N.N.; et al. Point-of-Care Breath Test for Biomarkers of Active Pulmonary Tuberculosis. *Tuberculosis* **2012**, *92*, 314–320. [CrossRef]

298. Lorwongtragool, P.; Sowade, E.; Watthanawisuth, N.; Baumann, R.; Kerdcharoen, T. A Novel Wearable Electronic Nose for Healthcare Based on Flexible Pinted Chemical Sensor Array. *Sensors* **2014**, *14*, 19700–19712. [CrossRef]

299. Mansour, E.; Palzur, E.; Broza, Y.Y.; Saliba, W.; Kaisari, S.; Goldstein, P.; Shamir, A.; Haick, H. Noninvasive Detection of Stress by Biochemical Profiles from the Skin. *ACS Sens.* **2023**, *8*, 1339–1347. [CrossRef]

300. Tai, H.; Wang, S.; Duan, Z.; Jiang, Y. Evolution of Breath Analysis Based on Humidity and Gas Sensors: Potential and Challenges. *Sens. Actuators B Chem.* **2020**, *318*, 128104. [CrossRef]

301. Feller, J.F. Smart Plastics Group. Available online: http://www.smartplasticsgroup.com (accessed on 7 January 2025).

302. Kumar, B.; Castro, M.; Feller, J.F. Controlled Conductive Junction Gap for Chitosan-Carbon Nanotube Quantum Resistive Vapour Sensors. *J. Mater. Chem.* **2012**, *22*, 10656–10664. [CrossRef]

303. Kumar, B.; Castro, M.; Feller, J.F. Tailoring the Chemo-Resistive Response of Self-Assembled Polysaccharide-CNT Sensors by Chain Conformation at Tunnel Junctions. *Carbon* **2012**, *50*, 3627–3634. [CrossRef]

304. Kumar, B.; Feller, J.F.; Castro, M.; Lu, J. Conductive Bio-Polymer Nano-Composites (CPC): Chitosan-Carbon Nanotube Transducers Assembled via Spray Layer-by-Layer for Volatile Organic Compound Sensing. *Talanta* **2010**, *81*, 908–915. [CrossRef] [PubMed]

305. Kumar, B.; Castro, M.; Feller, J.F. Quantum Resistive Vapour Sensors Made of Polymer Coated Carbon Nanotubes Random Networks for Biomarkers Detection. *Chem. Sens.* **2013**, *3*, 20.

306. Feller, J.F.; Lu, J.; Zhang, K.; Kumar, B.; Castro, M.; Gatt, N.; Choi, H.J. Novel Architecture of Carbon Nanotube Decorated Poly(Methyl Methacrylate) Microbead Vapour Sensors Assembled by Spray Layer by Layer. *J. Mater. Chem.* **2011**, *21*, 4142–4149. [CrossRef]

307. Lu, J.; Feller, J.F.; Kumar, B.; Castro, M.; Kim, Y.S.; Park, Y.T.; Grunlan, J.C. Chemo-Sensitivity of Latex-Based Films Containing Segregated Networks of Carbon Nanotubes. *Sens. Actuators B Chem.* **2011**, *155*, 28–36. [CrossRef]

308. Lu, J.; Park, B.J.; Kumar, B.; Castro, M.; Choi, H.J.; Feller, J.F. Polyaniline Nanoparticle-Carbon Nanotube Hybrid Network Vapour Sensors with Switchable Chemo-Electrical Polarity. *Nanotechnology* **2010**, *21*, 255501. [CrossRef]

309. Lu, J.; Kumar, B.; Castro, M.; Feller, J.F. Vapour Sensing with Conductive Polymer Nanocomposites (CPC): Polycarbonate-Carbon Nanotubes Transducers with Hierarchical Structure Processed by Spray Layer by Layer. *Sens. Actuators B Chem.* **2009**, *140*, 451–460. [CrossRef]

310. Chatterjee, S.; Castro, M.; Feller, J.F. An E-Nose Made of Carbon Nanotube Based Quantum Resistive Sensors for the Detection of Eighteen Polar/Nonpolar VOC Biomarkers of Lung Cancer. *J. Mater. Chem. B* **2013**, *1*, 4563. [CrossRef]

311. Chatterjee, S.; Castro, M.; Feller, J.F. Tailoring Selectivity of Sprayed Carbon Nanotube Sensors (CNT) towards Volatile Organic Compounds (VOC) with Surfactants. *Sens. Actuators B Chem.* **2015**, *220*, 840–849. [CrossRef]

312. Nag, S.; Duarte, L.; Bertrand, E.; Celton, V.; Castro, M.; Choudhary, V.; Guégan, P.; Feller, J.F. Ultrasensitive QRS Made by Supramolecular Assembly of Functionalized Cyclodextrins and Graphene for the Detection of Lung Cancer VOC Biomarkers. *J. Mater. Chem. B Biol. Med.* **2014**, *2*, 6571–6579. [CrossRef] [PubMed]

313. Nag, S.; Castro, M.; Choudhary, V.; Feller, J.F. Sulfonated Poly(Ether Ether Ketone) [SPEEK] Nanocomposites Based on Hybrid Nanocarbons for the Detection and Discrimination of Some Lung Cancer VOC Biomarkers. *J. Mater. Chem. B Biol. Med.* **2017**, *5*, 348–359. [CrossRef] [PubMed]

314. Nag-Chowdhury, S.; Tung, T.T.; Ta, Q.T.H.; Kumar, G.; Castro, M.; Feller, J.F.; Sonkar, S.K.; Tripathi, K.M. Upgrading of Diesel Engine Exhaust Waste into Onion-like Carbon Nanoparticles for Integrated Degradation Sensing in Nano-Biocomposites. *New J. Chem.* **2021**, *45*, 3675–3682. [CrossRef]

315. Duan, Y.; Pirolli, L.; Teplyakov, A.V. Investigation of the H2S Poisoning Process for Sensing Composite Material Based on Carbon Nanotubes and Metal Oxides. *Sens. Actuators B Chem.* **2016**, *235*, 213–221. [CrossRef] [PubMed]

316. Gathright, R.; Mejia, I.; Gonzalez, J.M.; Hernandez Torres, S.I.; Berard, D.; Snider, E.J. Overview of Wearable Healthcare Devices for Clinical Decision Support in the Prehospital Setting. *Sensors* **2024**, *24*, 8204. [CrossRef]

317. Jin, H.; Yu, J.; Lin, S.; Gao, S.; Yang, H.; Haick, H.; Hua, C.; Deng, S.; Yang, T.; Liu, Y.; et al. Nanosensor-Based Flexible Electronic Assisted with Light Fidelity Communicating Technology for Volatolomics-Based Telemedicine. *ACS Nano* **2020**, *14*, 15517–15532. [CrossRef]

318. Sood, A.; Granick, M.S.; Trial, C.; Lano, J.; Palmier, S.; Ribal, E.; Téot, L. The Role of Telemedicine in Wound Care: A Review and Analysis of a Database of 5795 Patients from a Mobile Wound-Healing Center in Languedoc-Roussillon, France. *Plast. Reconstr. Surg.* **2016**, *138*, 248S–256S. [CrossRef]